APPENDIX A

CAI RESULTS FOR INTACT ROCK

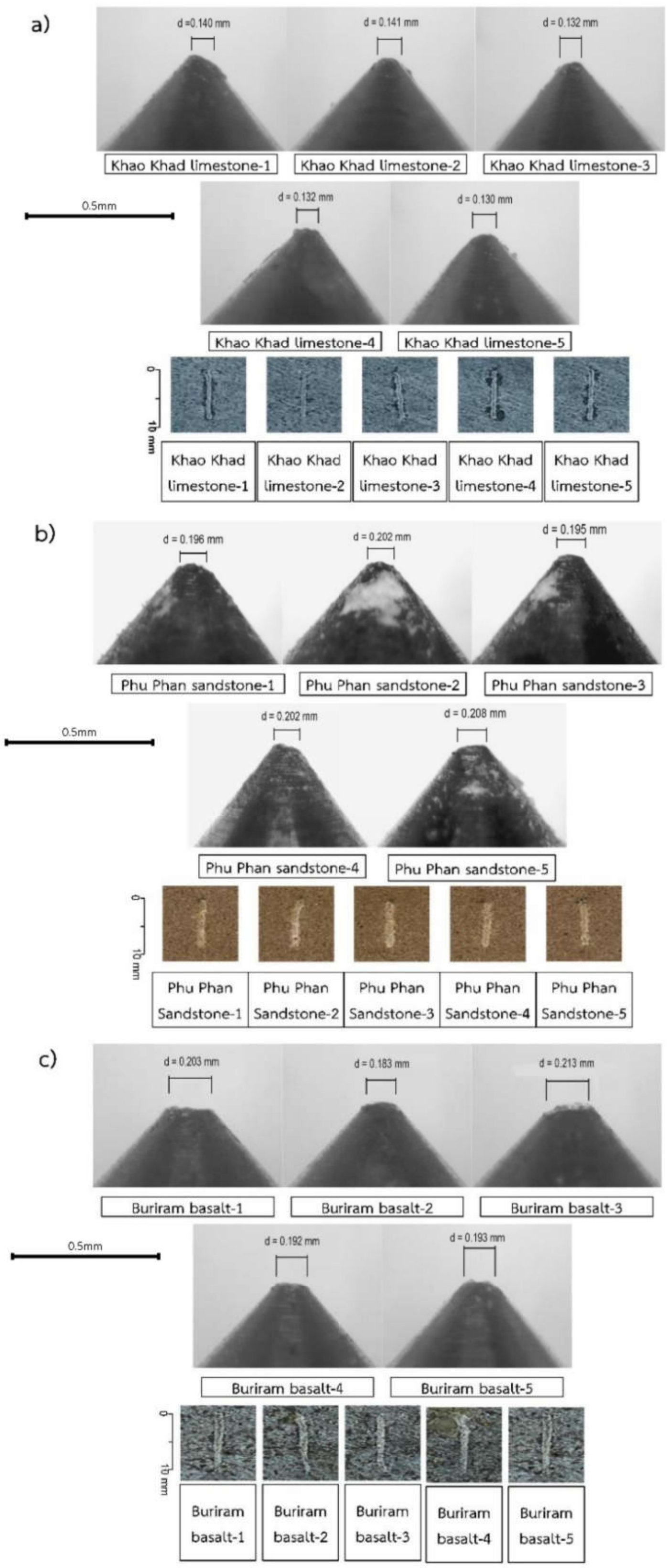

Figure A.1 Stylus tips after CERCHAR testing and scratching trace after testing on intact rock

APPENDIX B

CAI RESULTS FOR ONE JOINT WITH DIFFERENT APERTURES

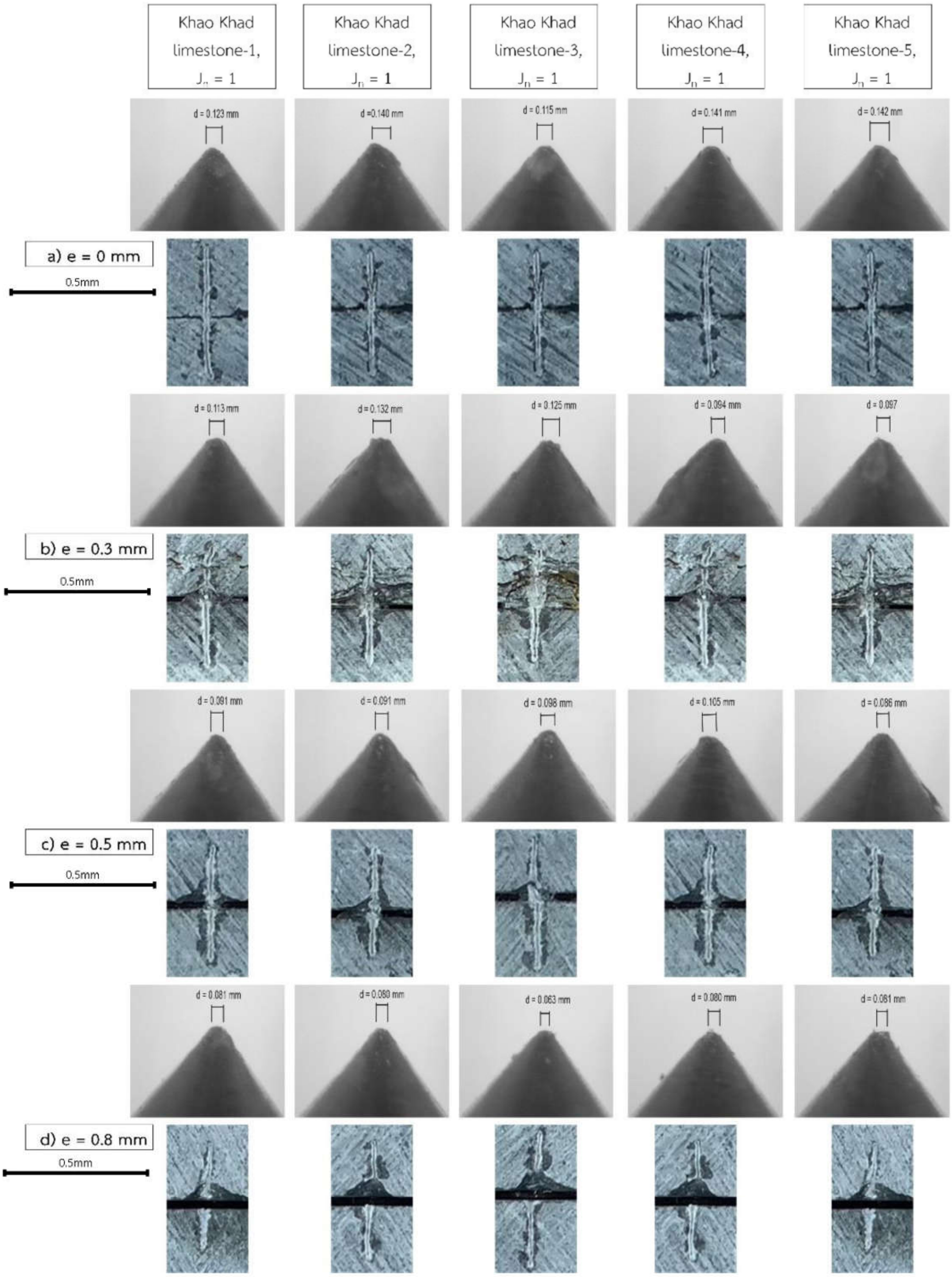

Figure B.1 CAI results for one joint with different apertures of Khao Khad limestone for apertures of 0 mm (a), 0.3 mm (b), 0.5 mm (c) and 0.8 mm (d).

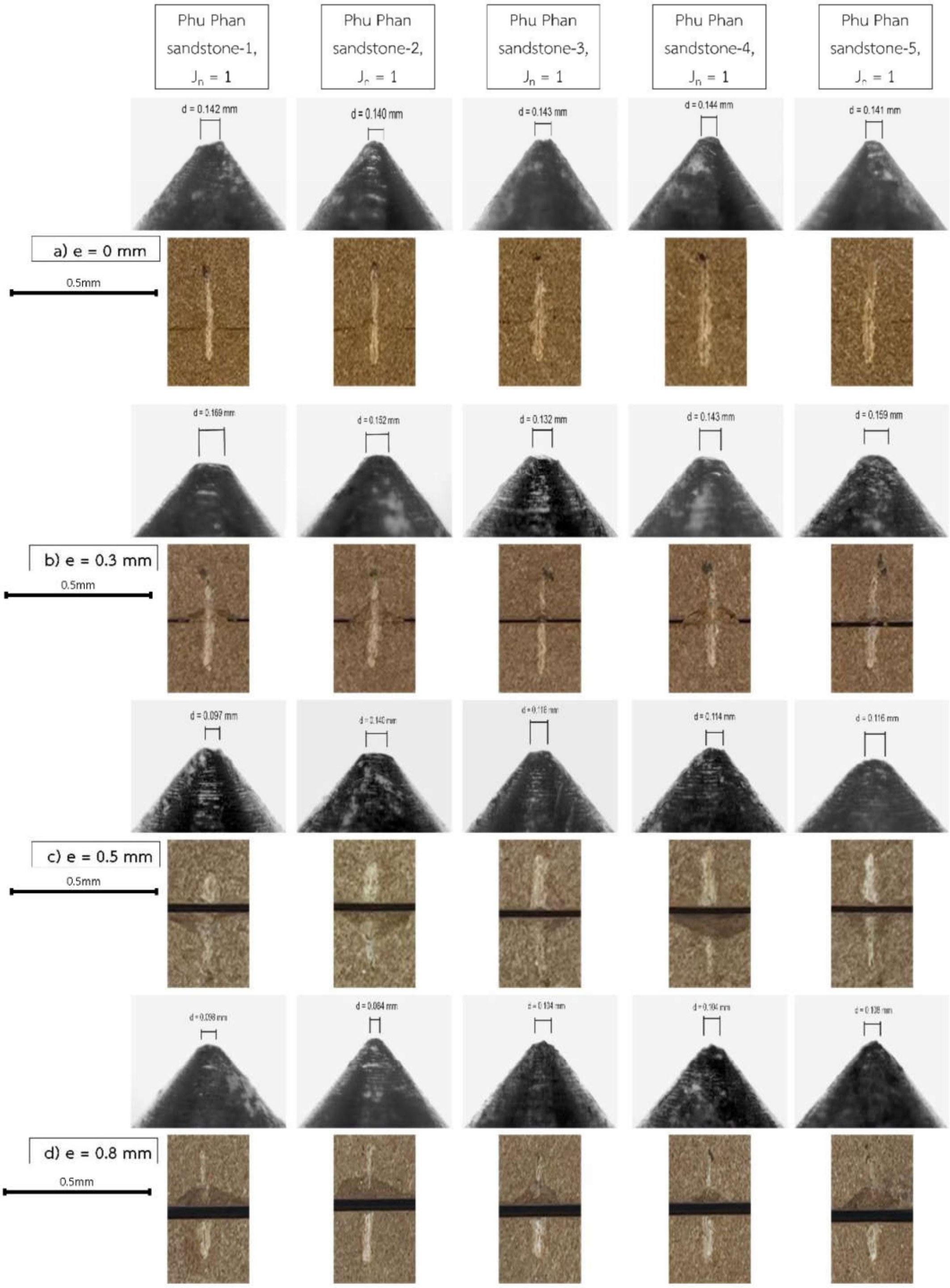

Figure B.2 CAI results for one joint with different apertures of Phu Phan sandstone for apertures of 0 mm (a), 0.3 mm (b), 0.5 mm (c) and 0.8 mm (d).

.

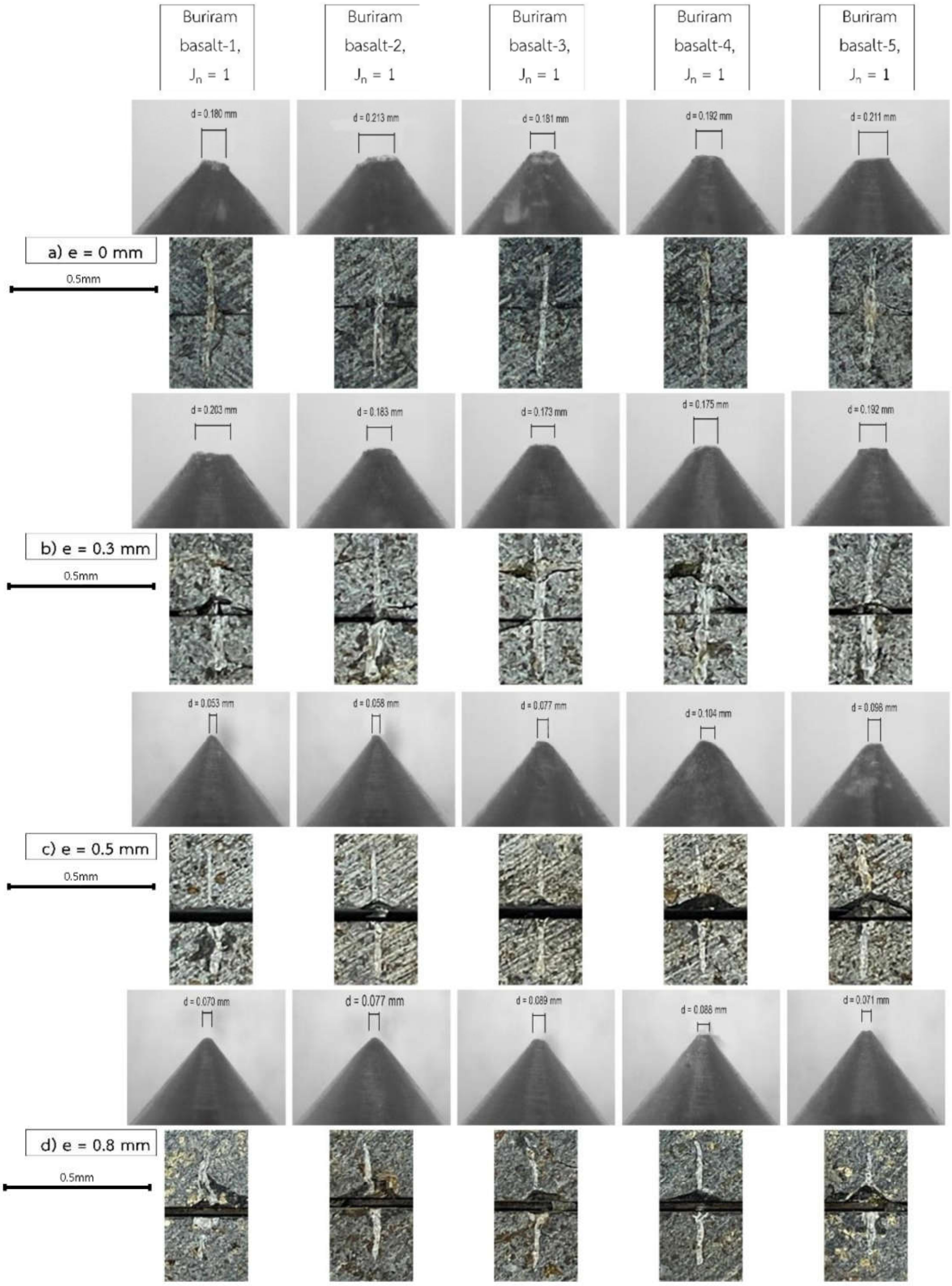

Figure B.3 CAI results for one joint with different apertures of Buriram basalt for apertures of 0 mm (a), 0.3 mm (b), 0.5 mm (c) and 0.8 mm (d).

.

APPENDIX C

CAI RESULTS FOR TWO JOINTS WITH DIFFERENT APERTURES

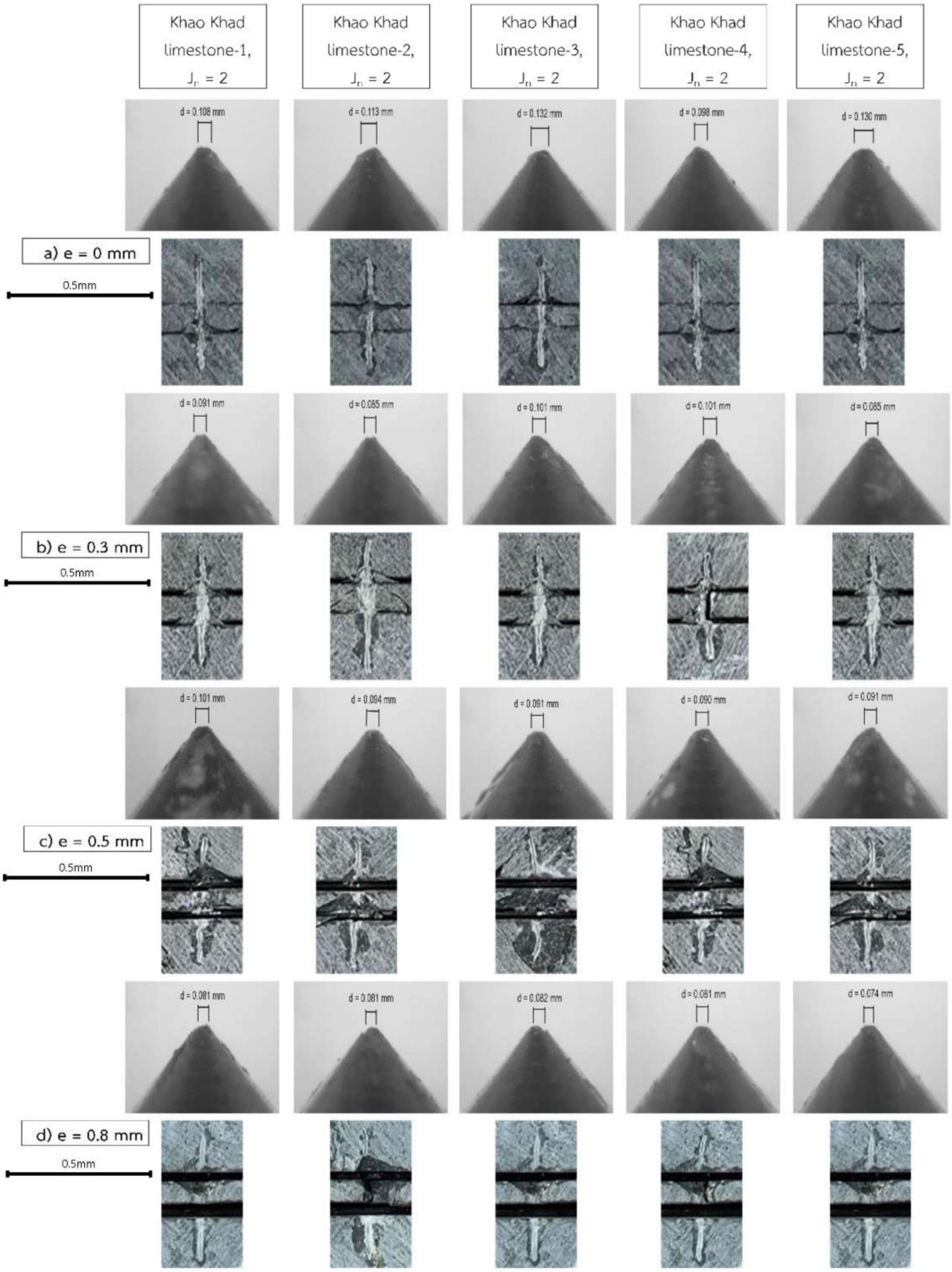

Figure C.1 CAI result for two joints with different aperture of Khao Khad limestone for aperture of 0 mm (a), 0.3 mm (b), 0.5 mm (c) and 0.8 mm (d).

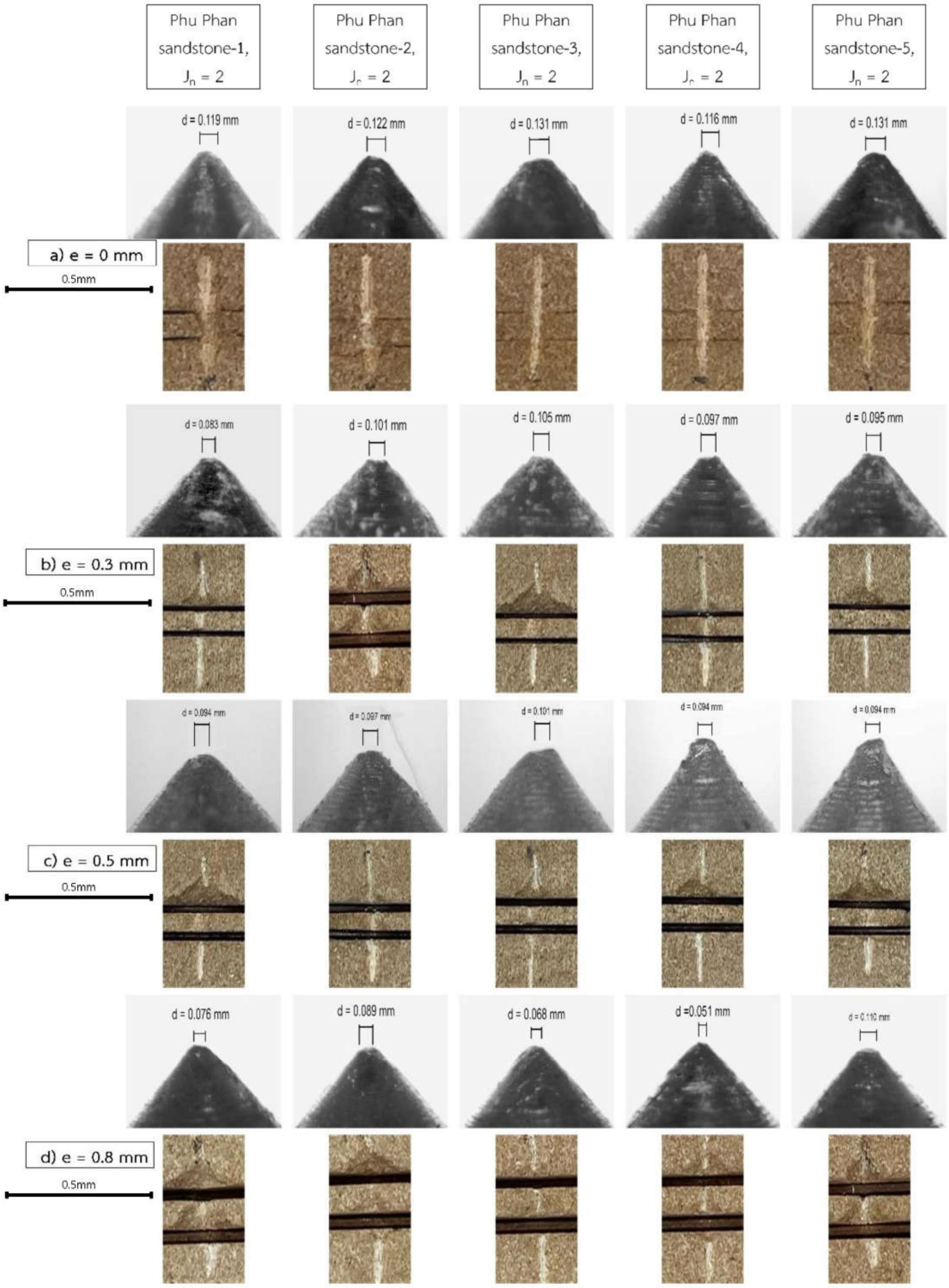

Figure C.2 CAI result for two joints with different aperture of Phu Phan sandstone for aperture of 0 mm (a), 0.3 mm (b), 0.5 mm (c) and 0.8 mm (d).

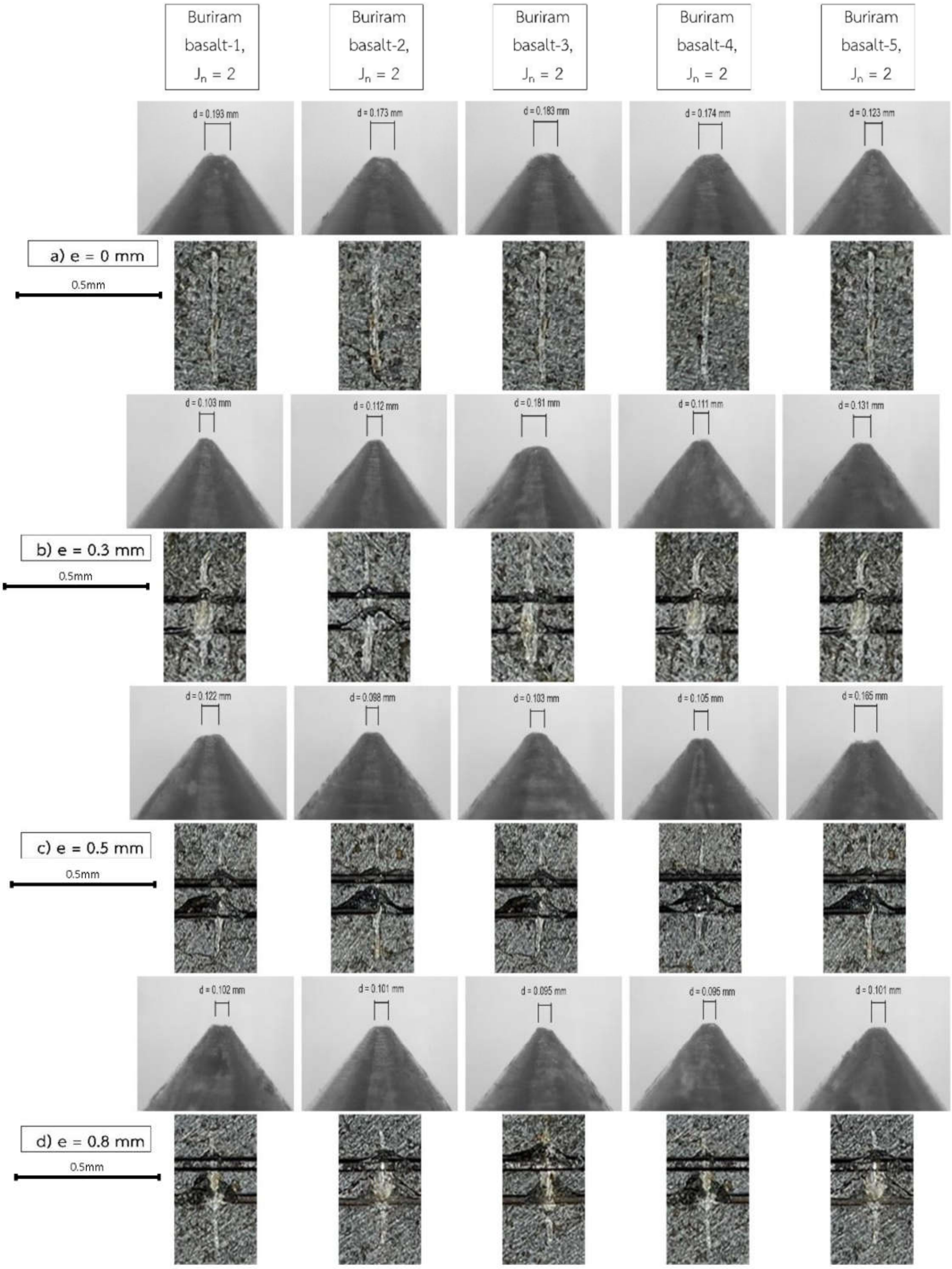

Figure C.3 CAI result for two joints with different aperture of Buriram basalt for aperture of 0 mm (a), 0.3 mm (b), 0.5 mm (c) and 0.8 mm (d).

APPENDIX D

CAI RESULTS FOR THREE JOINTS WITH DIFFERENT APERTURES

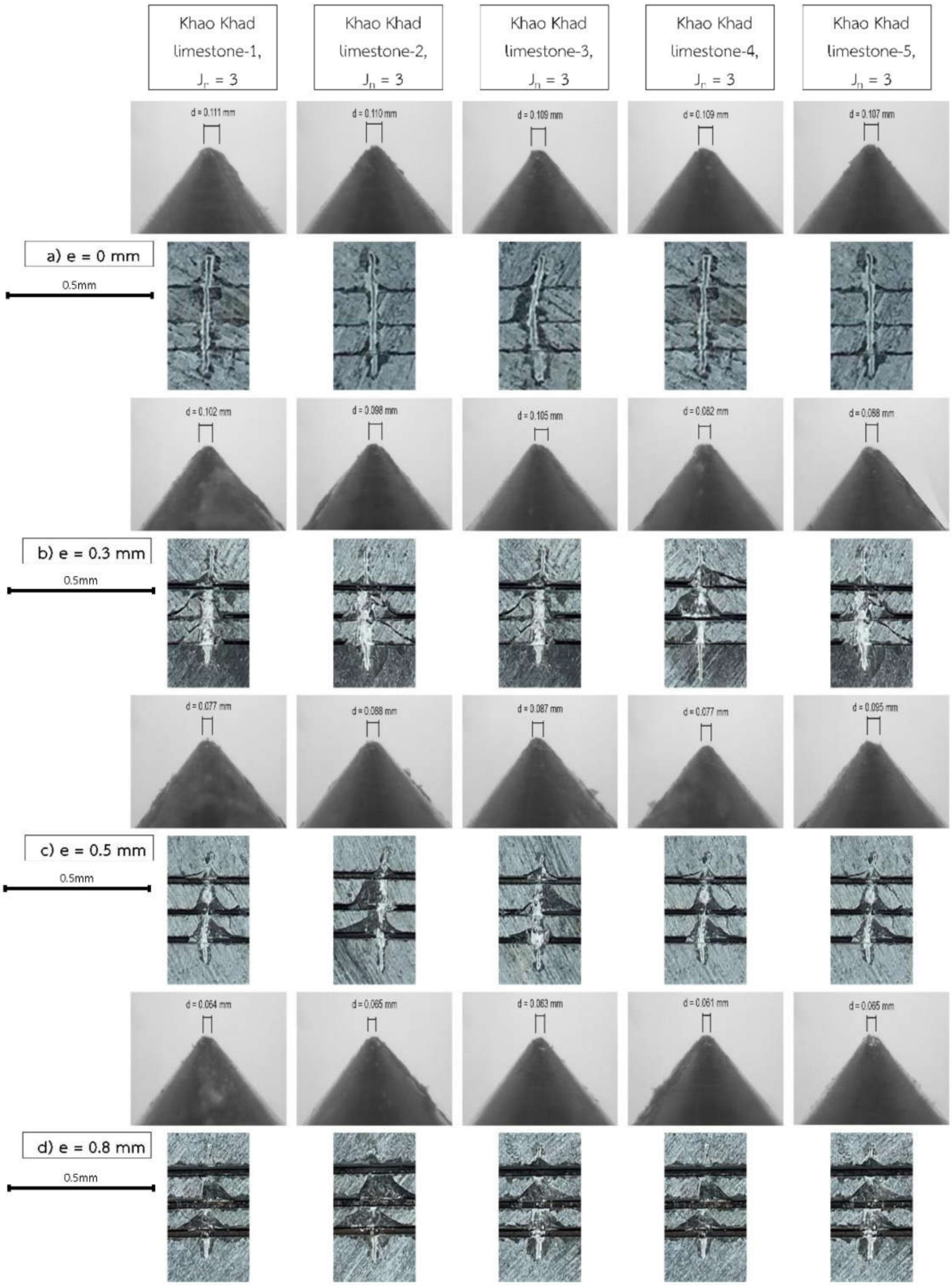

Figure D.1 CAI result for three joints with different aperture of Khao Khad limestone for aperture of 0 mm (a), 0.3 mm (b), 0.5 mm (c) and 0.8 mm (d).

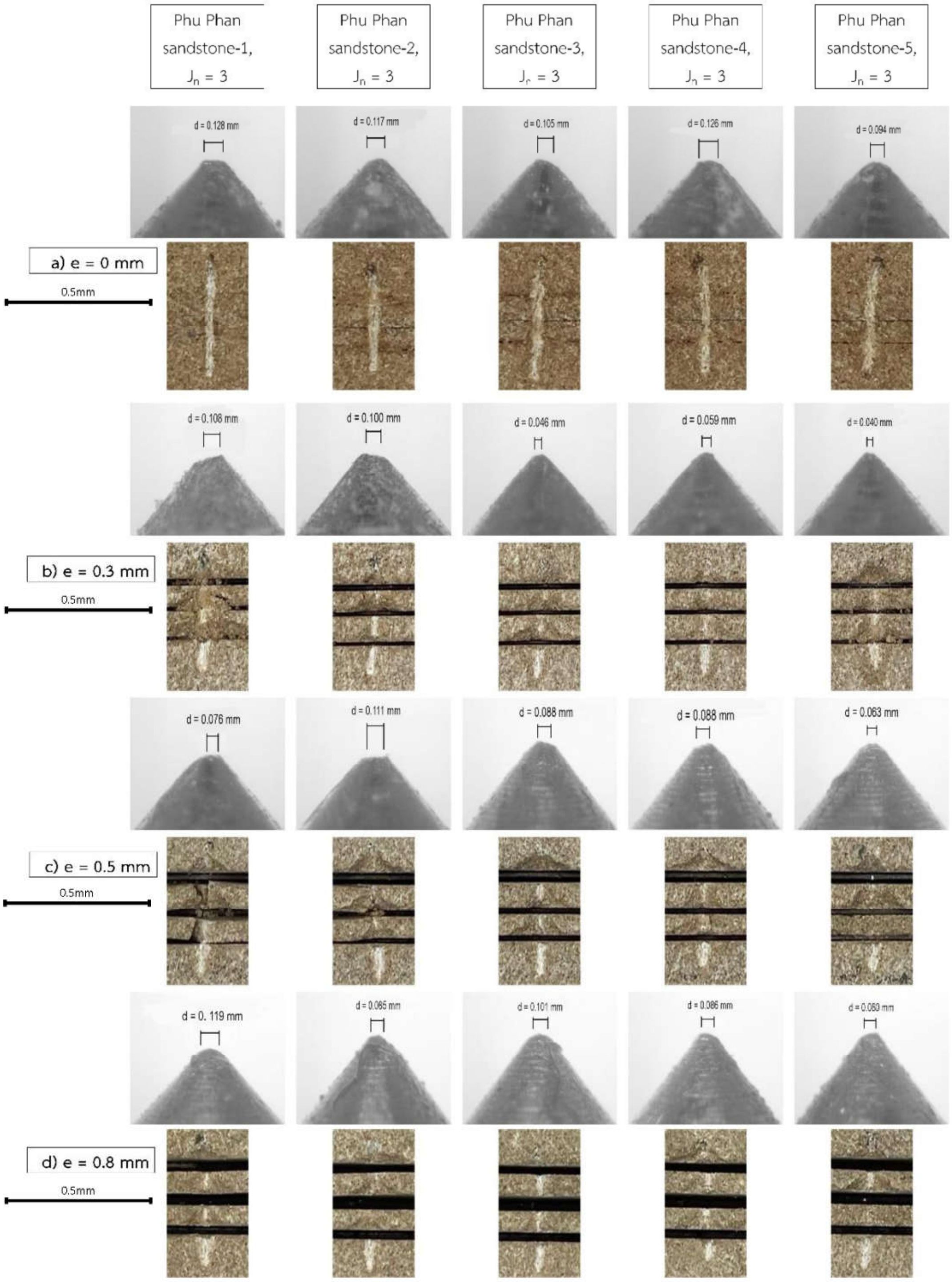

Figure D.2 CAI result for three joints with different aperture of Phu Phan sandstone for aperture of 0 mm (a), 0.3 mm (b), 0.5 mm (c) and 0.8 mm (d).

.

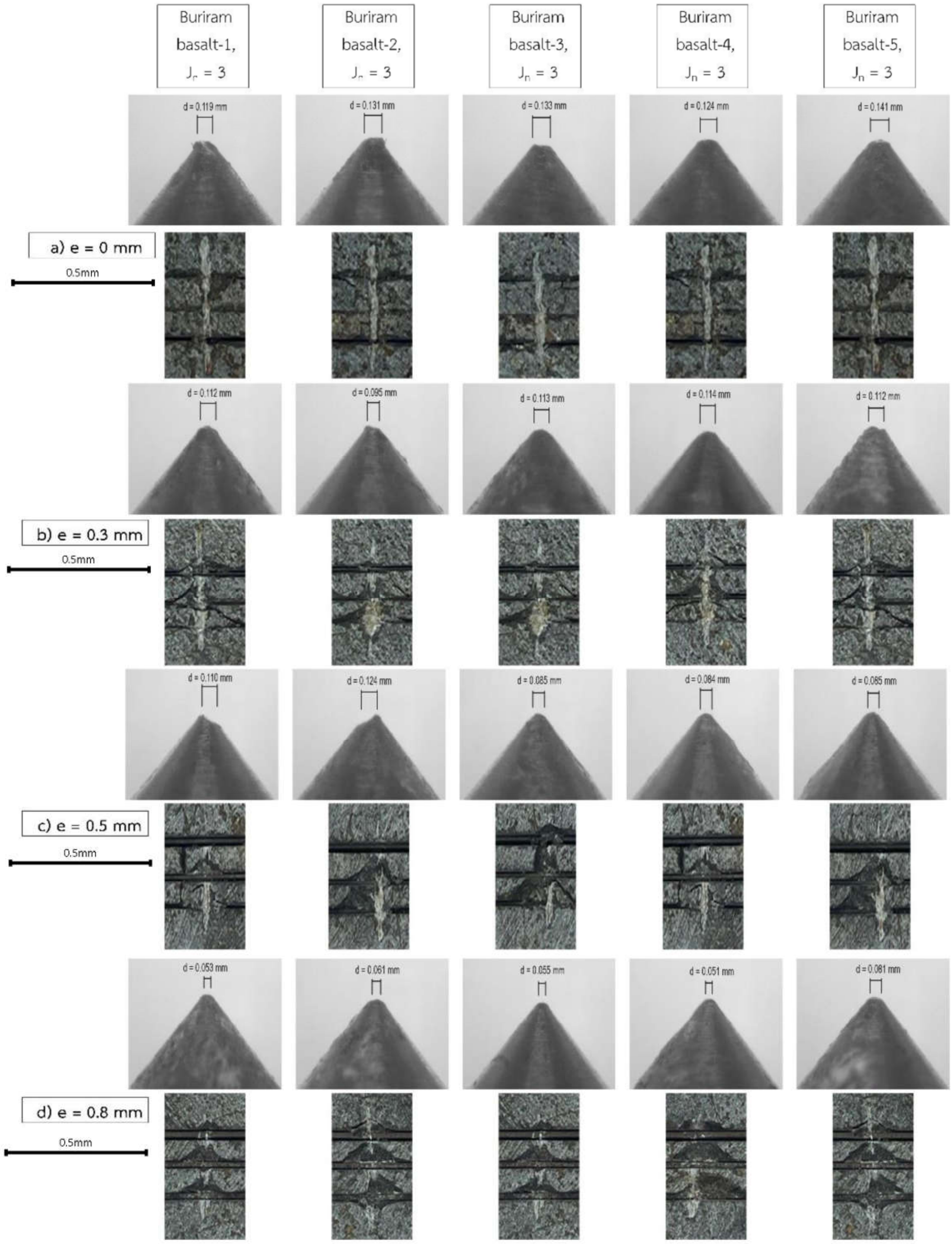

Figure D.3 CAI result for three joints with different aperture of Buriram basalt for aperture of 0 mm (a), 0.3 mm (b), 0.5 mm (c) and 0.8 mm (d).

.

APPENDIX E

CAI RESULTS FOR FOUR JOINTS WITH DIFFERENT APERTURES

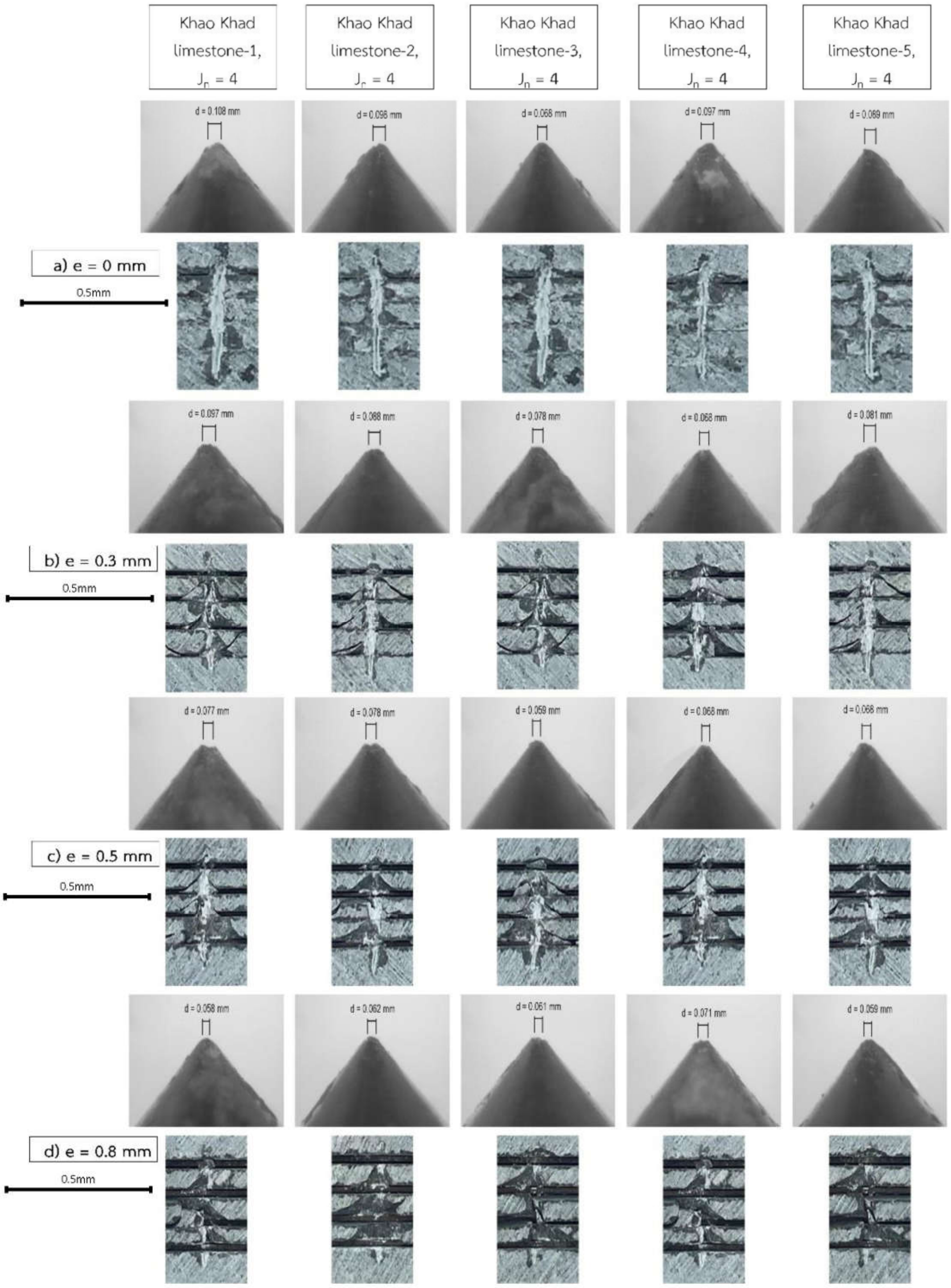

Figure E.1 CAI result for four joints with different aperture of Khao Khad limestone for aperture of 0 mm (a), 0.3 mm (b), 0.5 mm (c) and 0.8 mm (d).

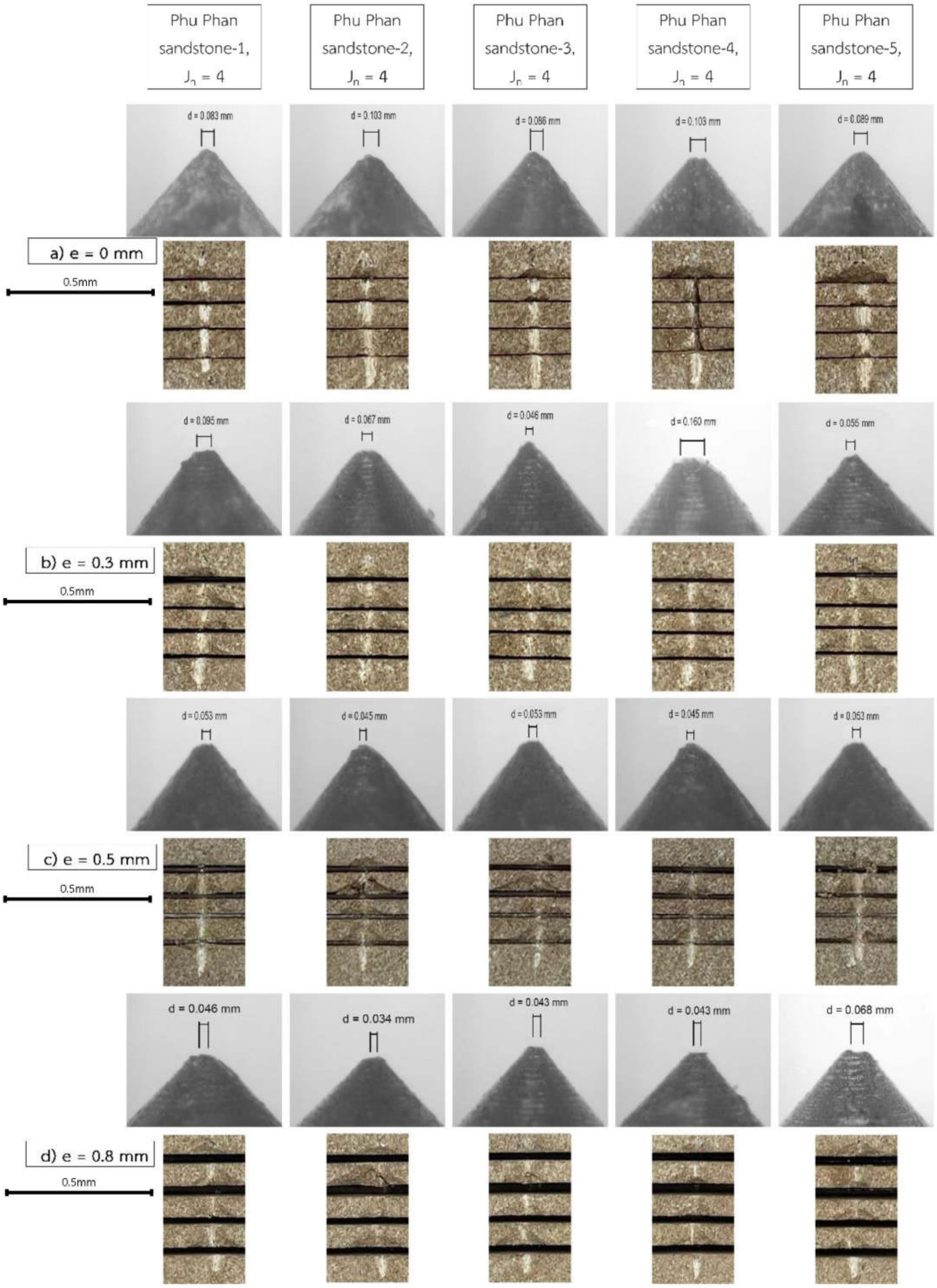

Figure E.2 CAI result for four joints with different aperture of Phu Phan sandstone for aperture of 0 mm (a), 0.3 mm (b), 0.5 mm (c) and 0.8 mm (d).

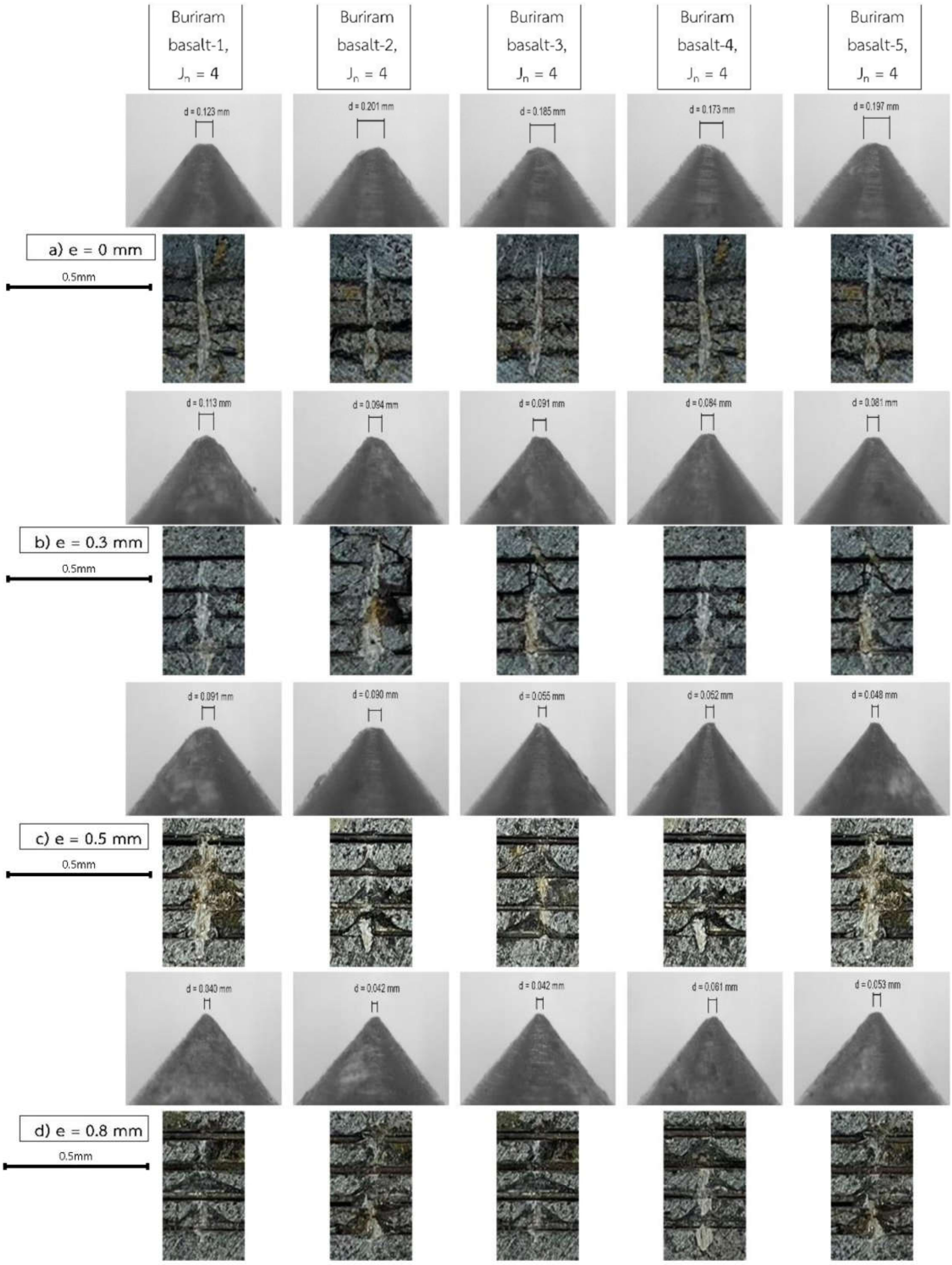

Figure E.3 CAI result for four joints with different aperture of Buriram basalt for aperture of 0 mm (a), 0.3 mm (b), 0.5 mm (c) and 0.8 mm (d).

APPENDIX F

LATERAL FORCE AS A FUNCTION OF SCRATCHING DISPLACEMENT

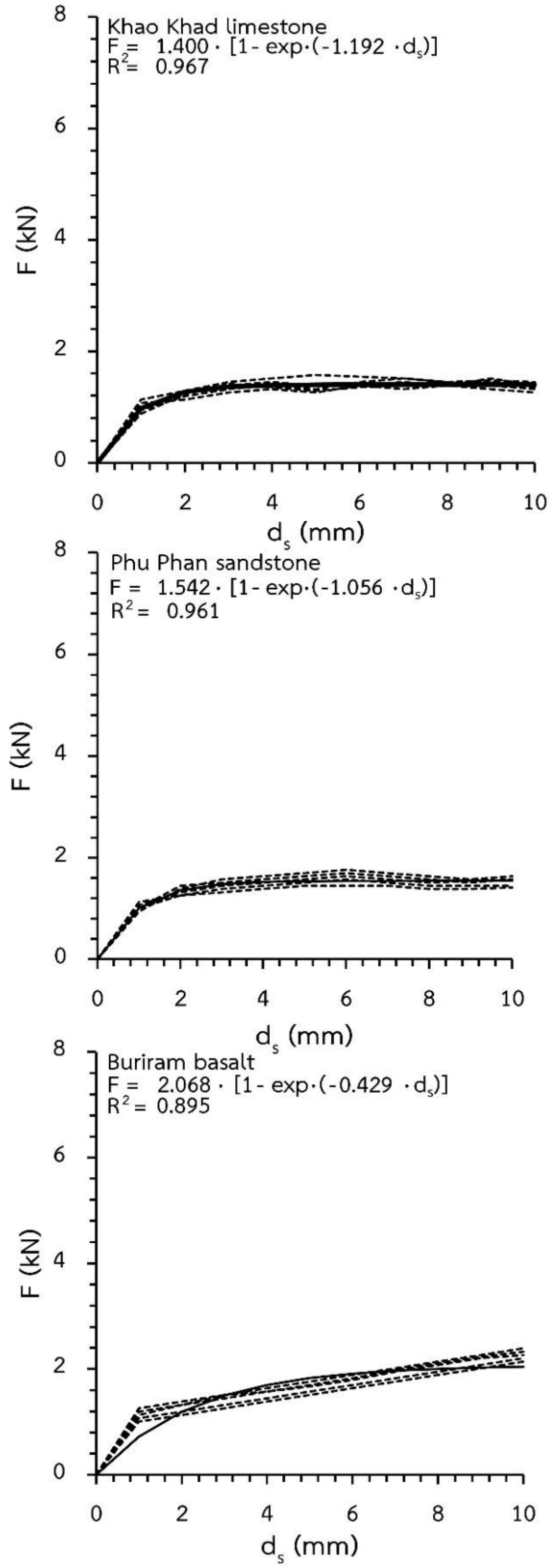

Figure F.1 Lateral force as a function of scratching displacement for Intact rock

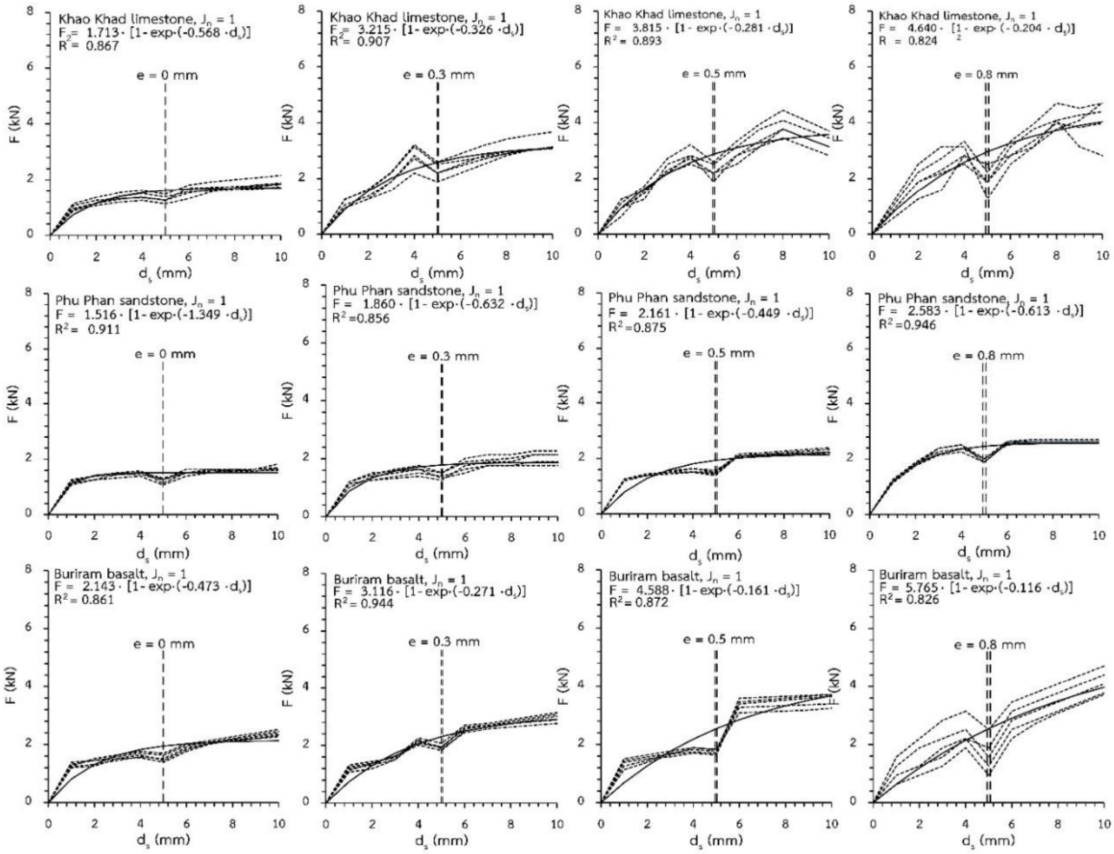

Figure F.2 Lateral force as a function of scratching displacement (d_s) for one joint specimens.

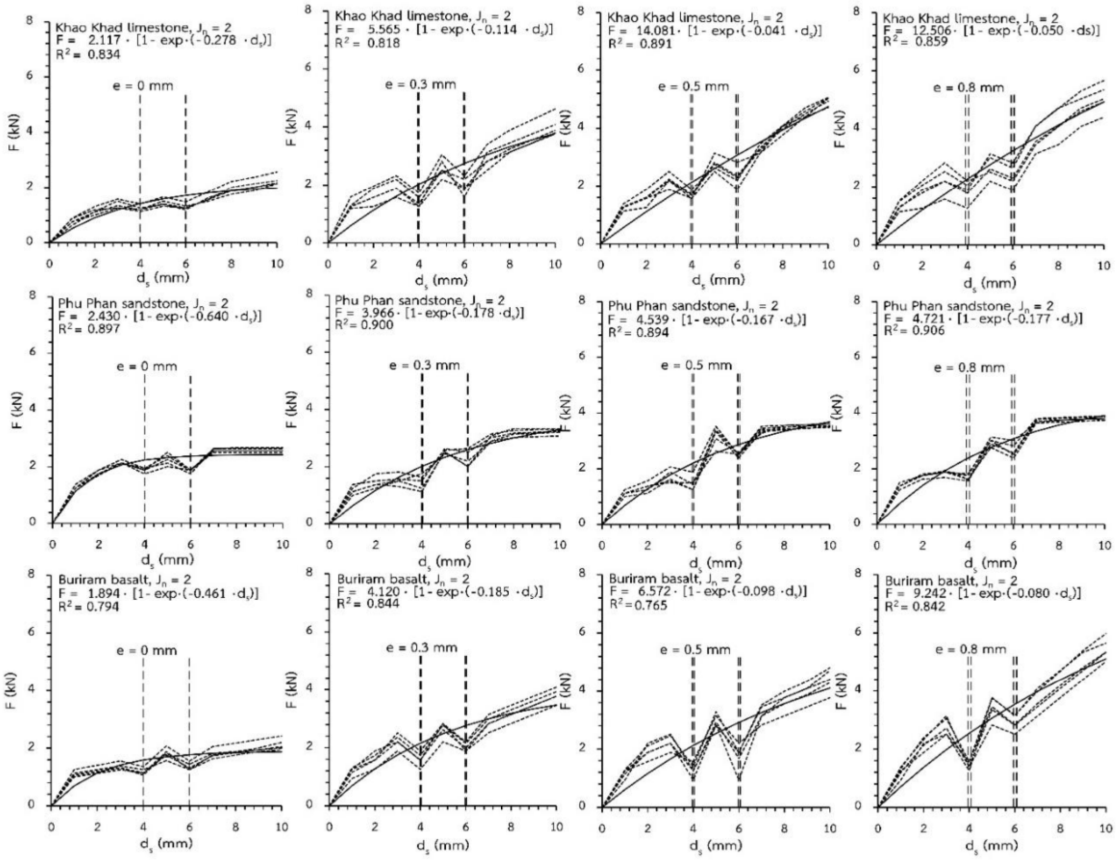

Figure F.3 Lateral force as a function of scratching displacement (d_s) for two joints specimens.

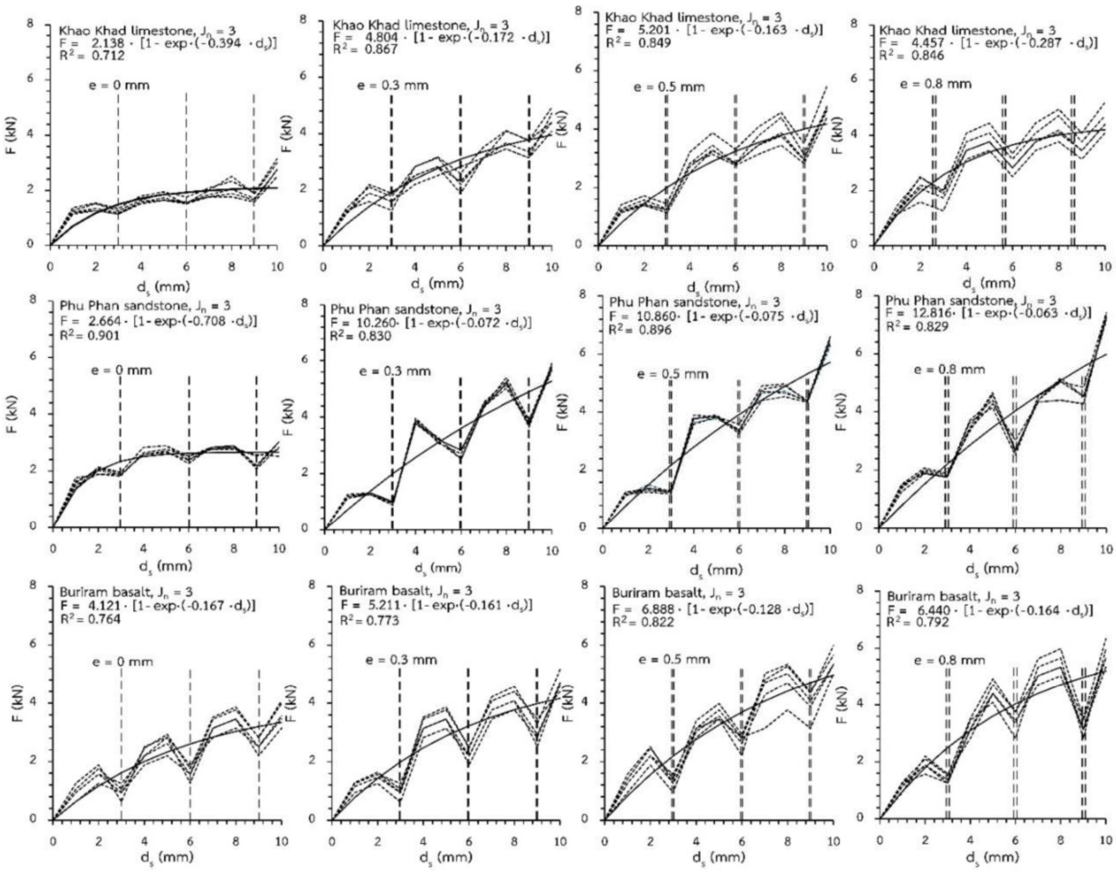

Figure F.4 Lateral force as a function of scratching displacement (d_s) for three joints specimens.

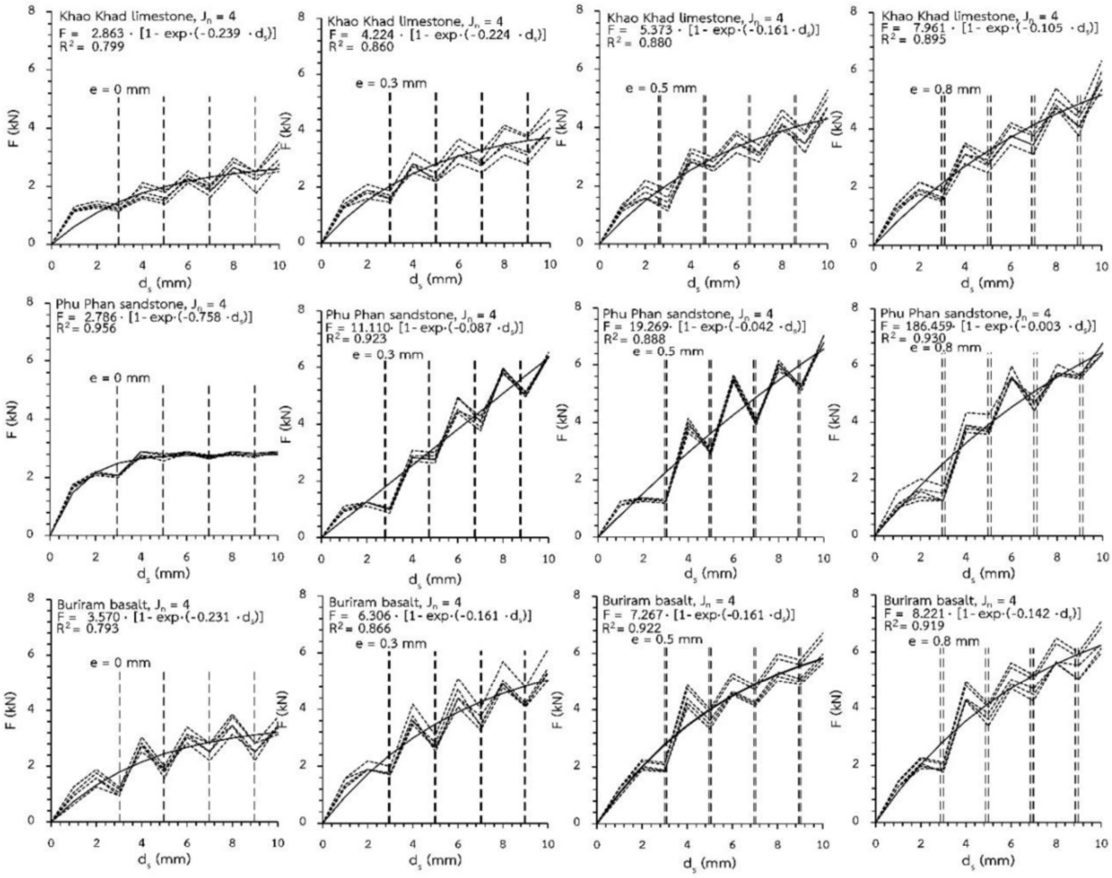

Figure F.5 Lateral force as a function of scratching displacement (d_S) for four joints specimens.

APPENDIX G

LASER - SCANNED IMAGES

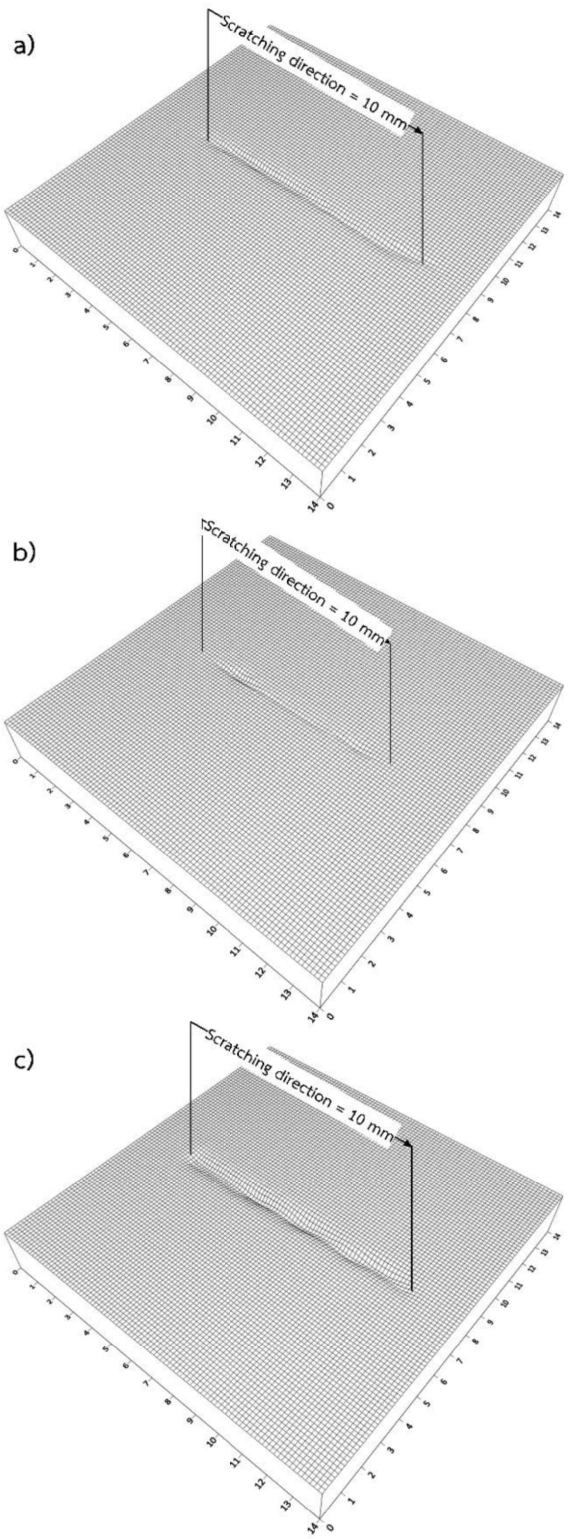

Figure G.1 Example of scratching groove profile on rock surfaces after CAI testing for intact rock for Khao Khad limestone (a), Phu Phan sandstone (b) and Buriram basalt (c). Arrow indicates scratching direction.

Khao Khad limestone, J_n = 1

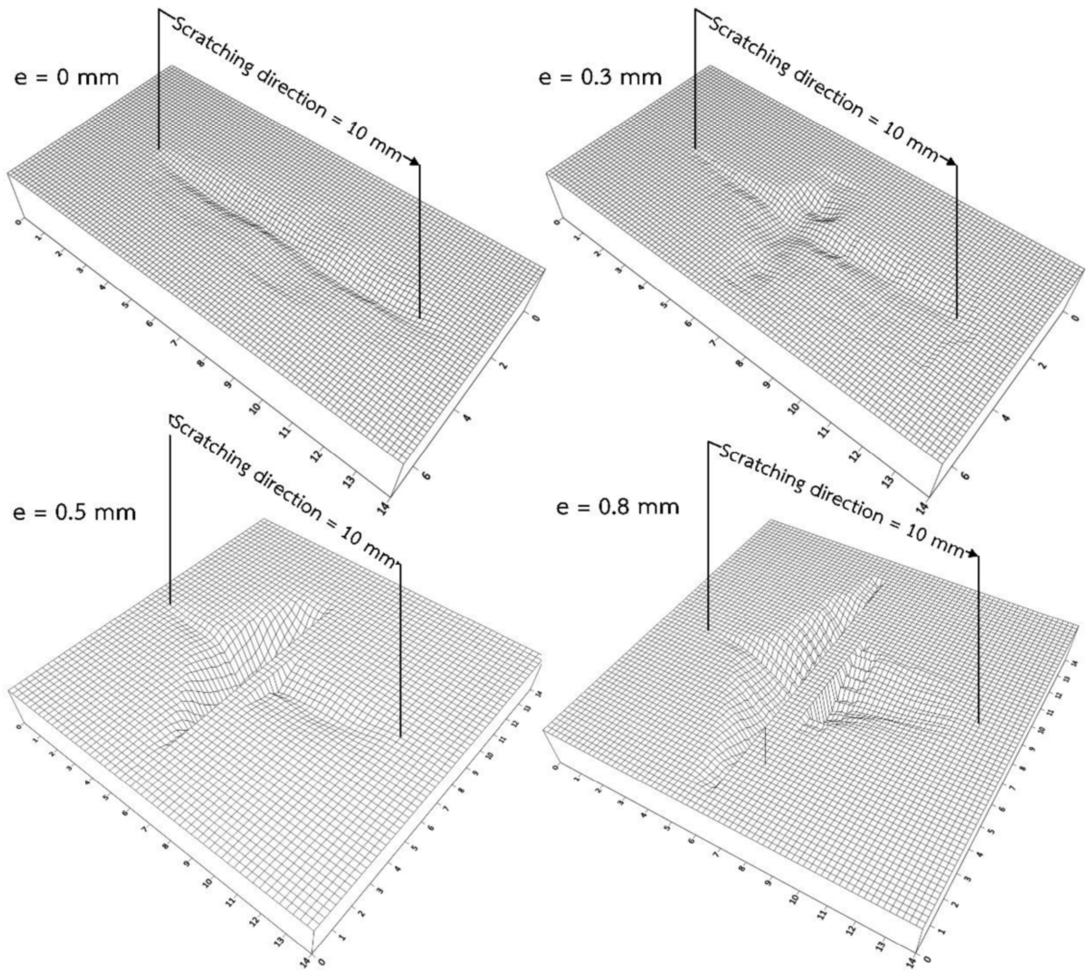

Figure G.2 Example of scratching groove profile on rock surfaces of Khao Khad limestone after CAI testing for one joint. Arrow indicates scratching direction.

Phu Phan sandstone, J_n = 1

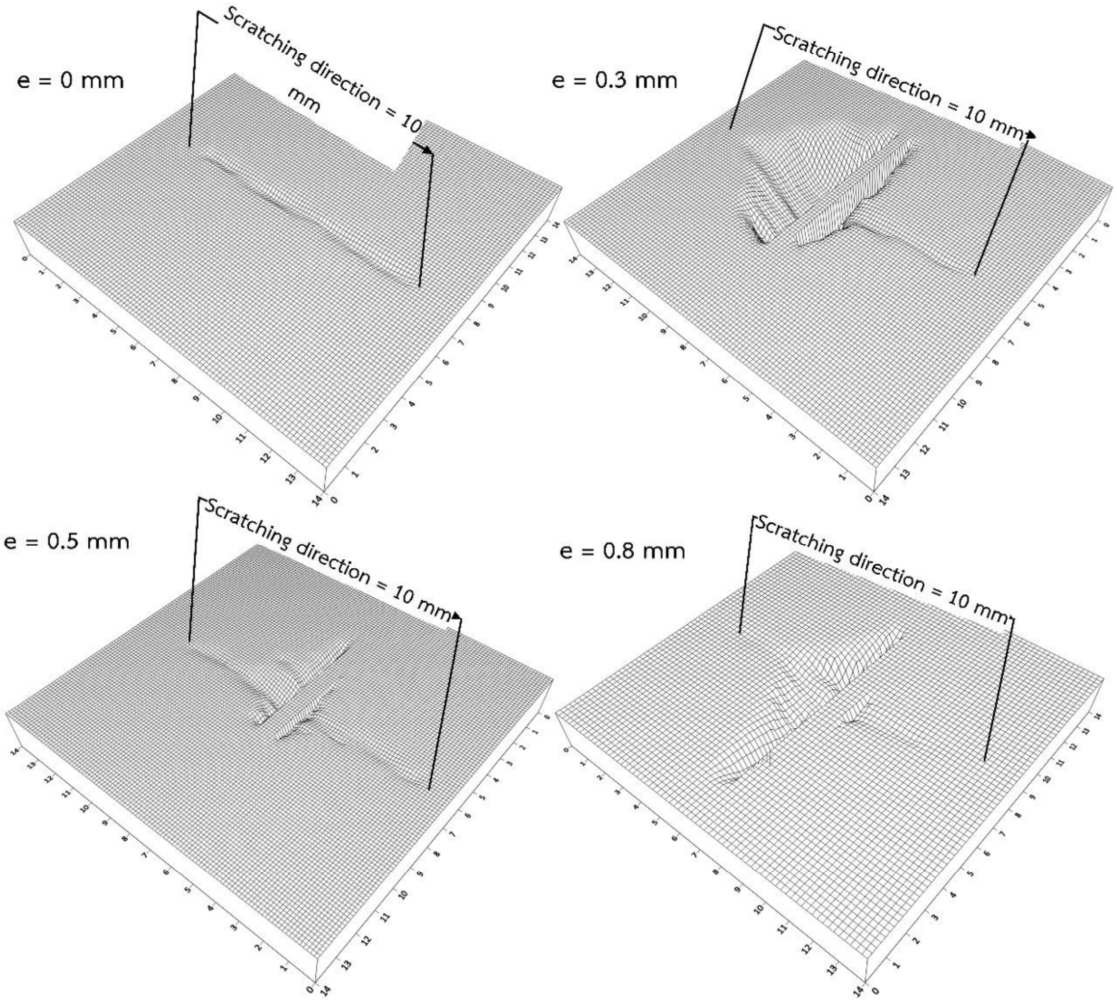

Figure G.3 Example of scratching groove profile on rock surfaces of Phu Phan sandstone after CAI testing for one joint. Arrow indicates scratching direction.

Buriram basalt, J_n = 1

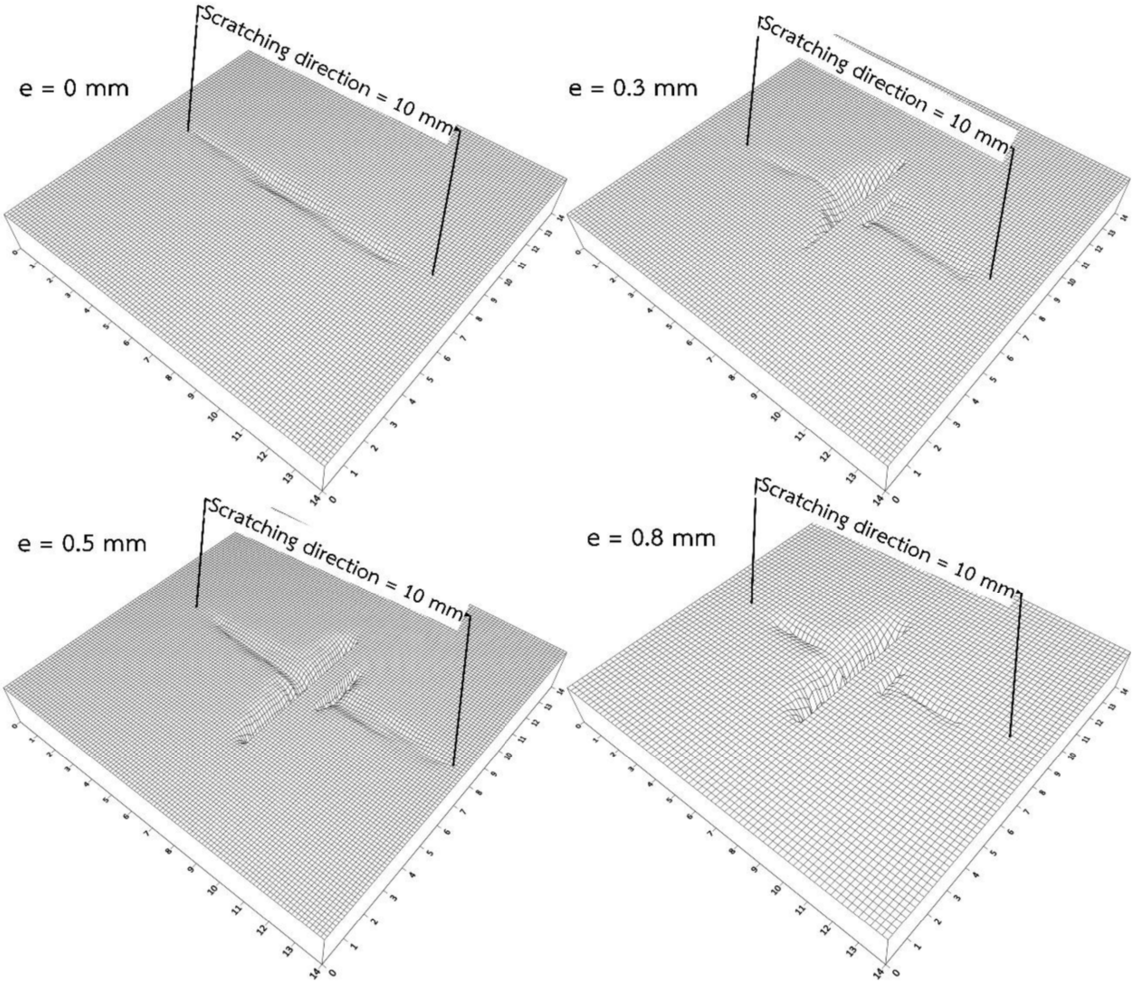

Figure G.4 Example of scratching groove profile on rock surfaces of Buriram basalt after CAI testing for one joint. Arrow indicates scratching direction.

Khao Khad limestone, J_n = 2

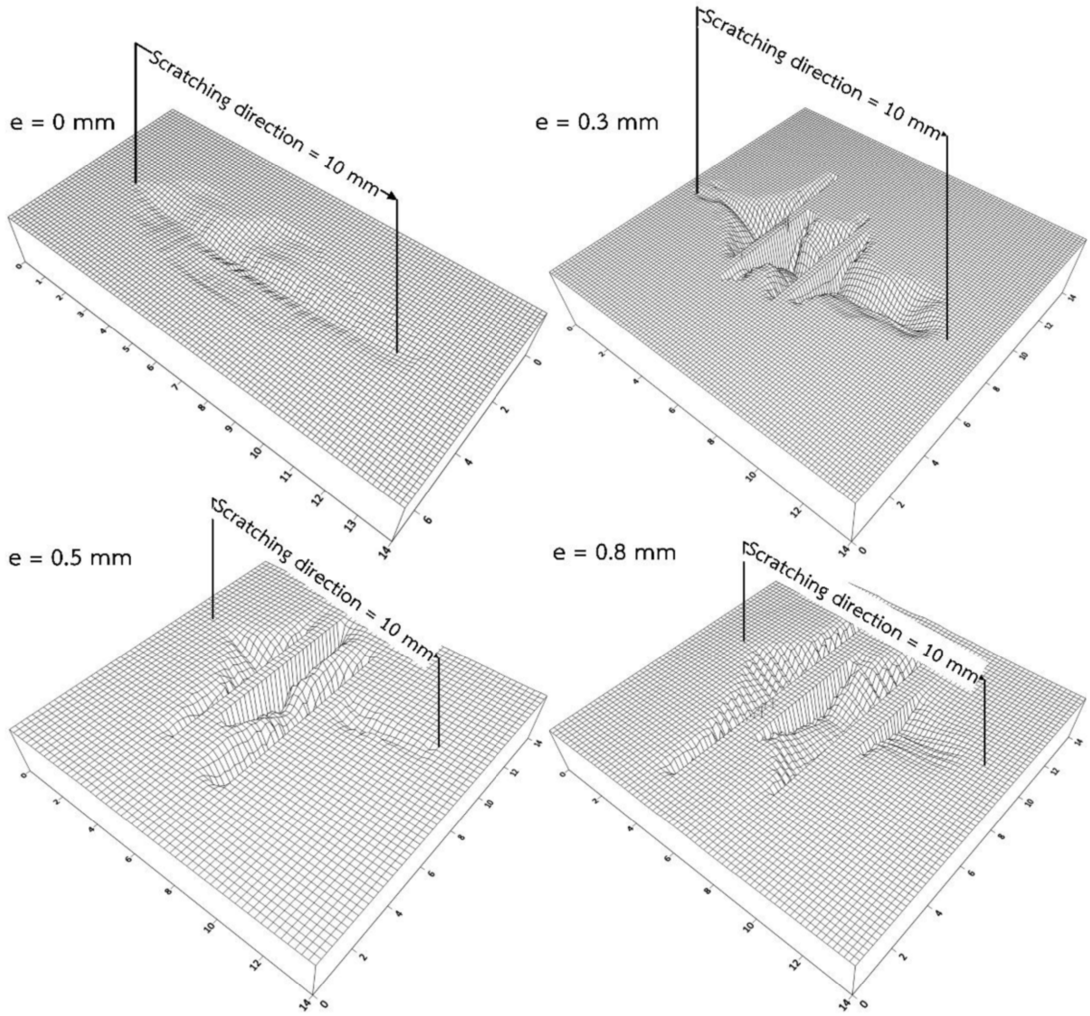

Figure G.5 Example of scratching groove profile on rock surfaces of Khao Khad limestone after CAI testing for two joints. Arrow indicates scratching direction.

Phu Phan sandstone, J_n = 2

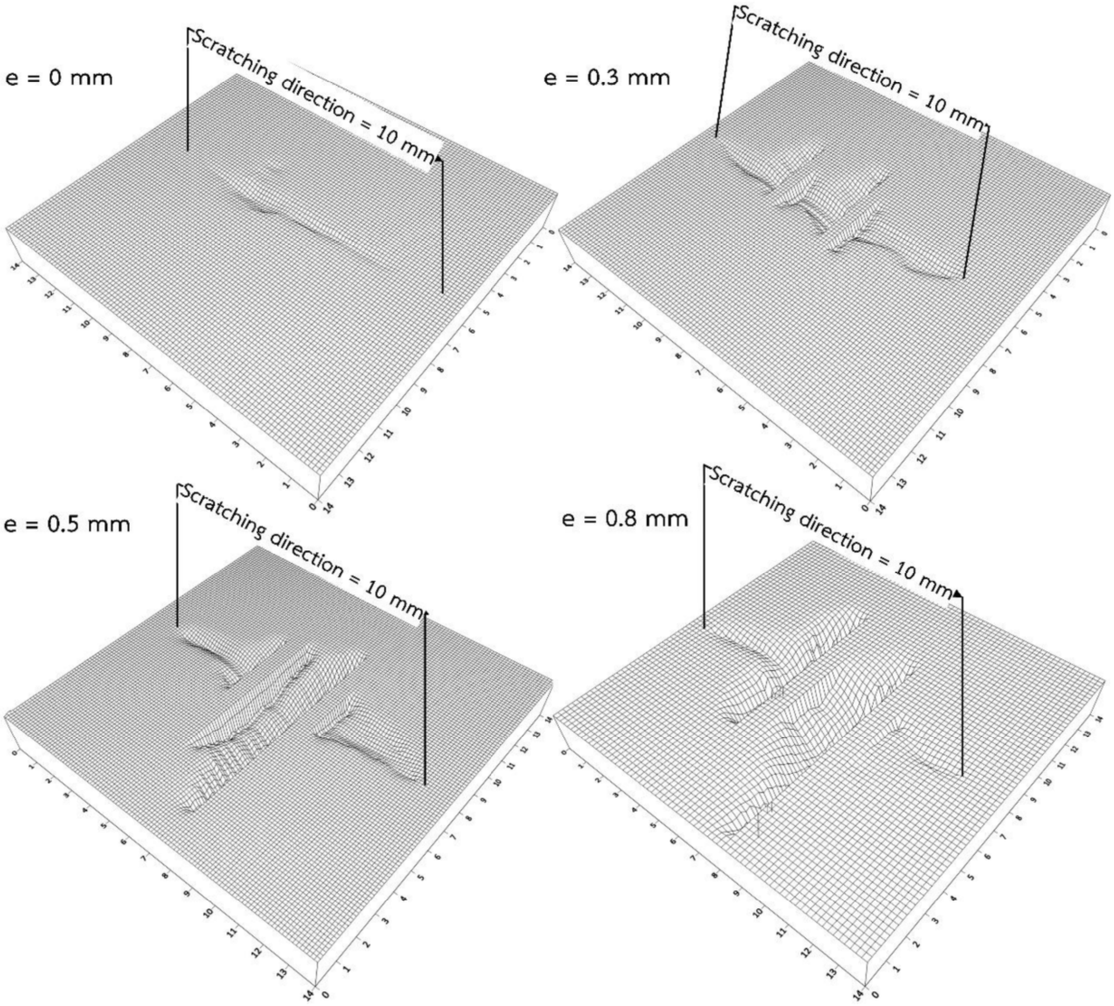

Figure G.6 Example of scratching groove profile on rock surfaces of Phu Phan sandstone after CAI testing for two joints. Arrow indicates scratching direction.

Buriram basalt, J_n = 2

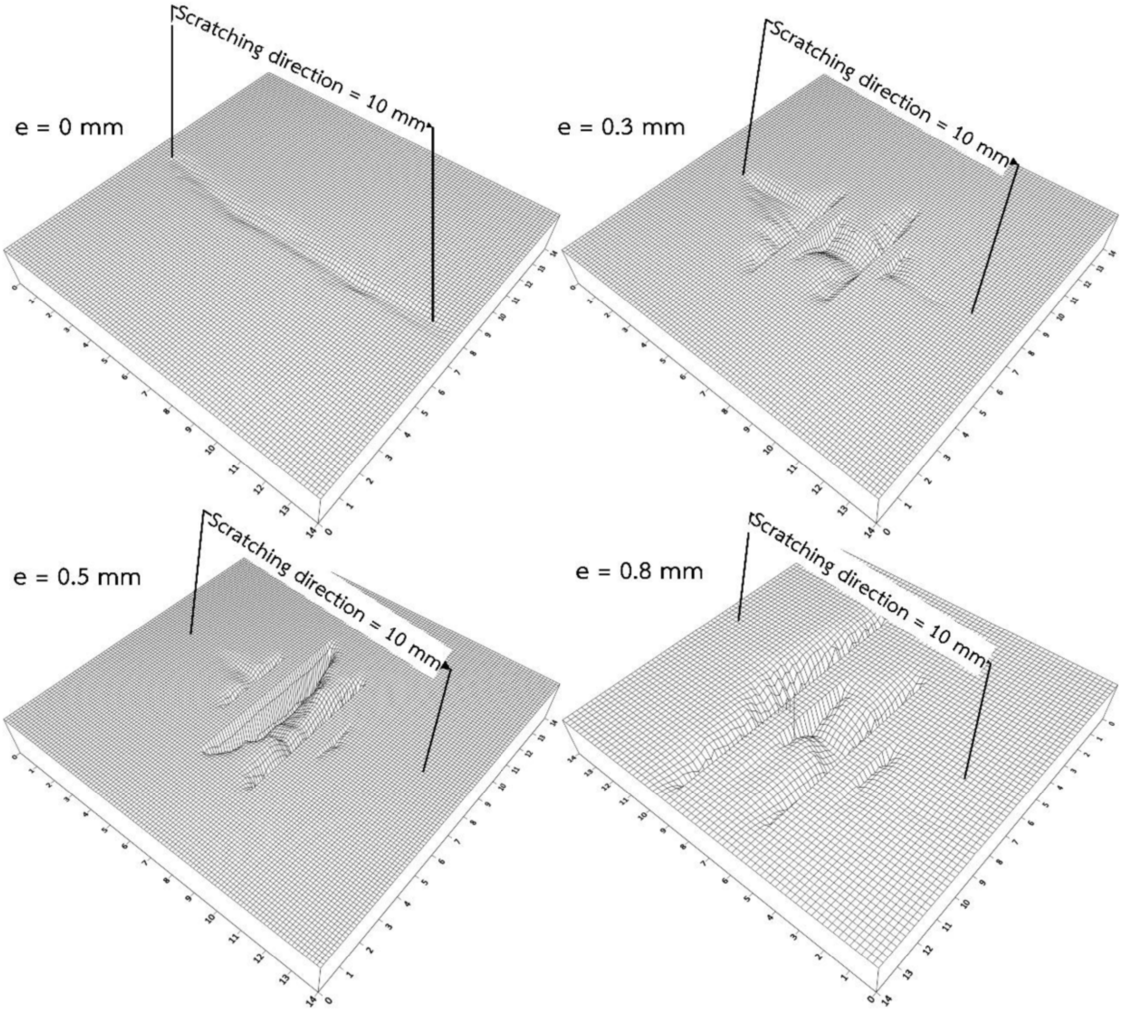

Figure G.7 Example of scratching groove profile on rock surfaces of Buriram basalt after CAI testing for two joints. Arrow indicates scratching direction.

Khao Khad limestone, J_n = 3

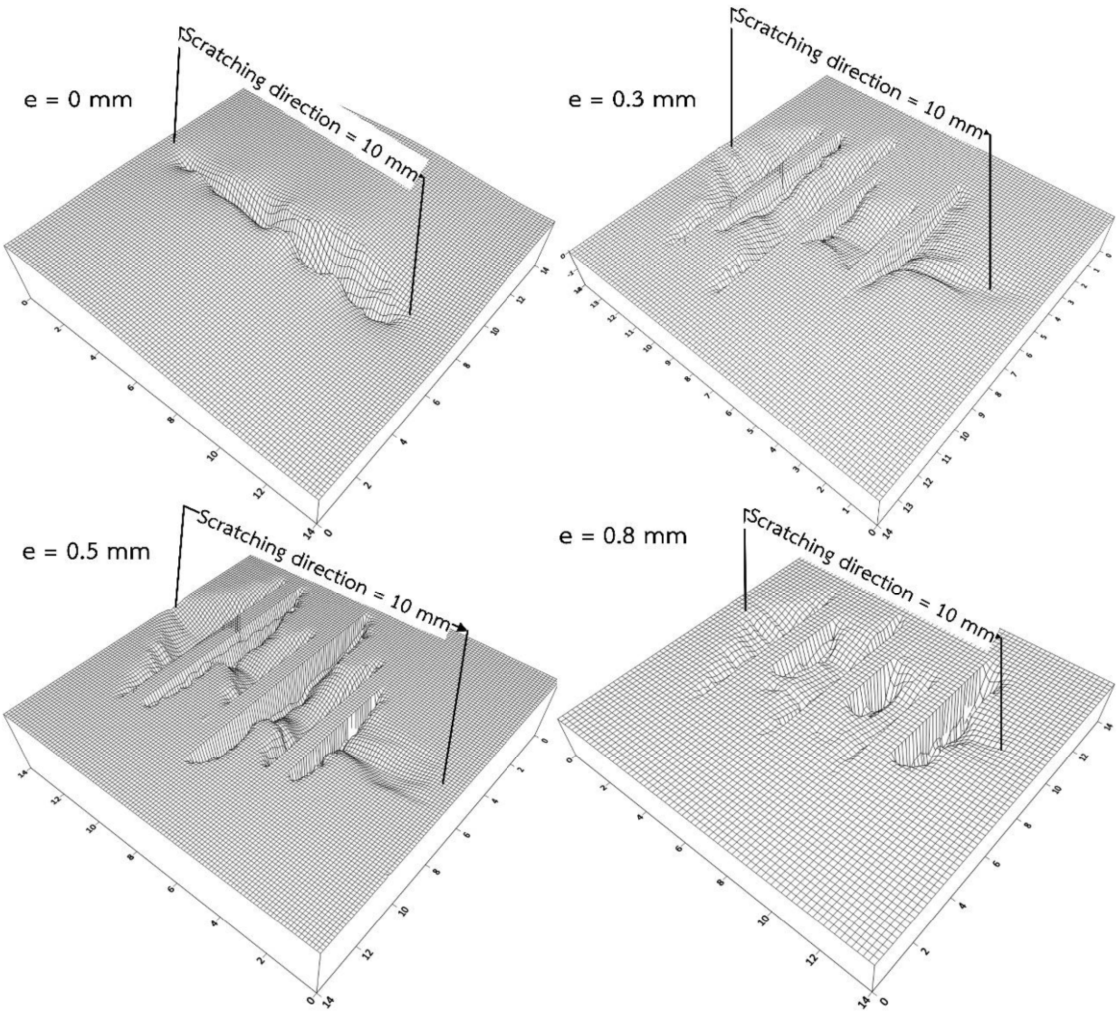

Figure G.8 Example of scratching groove profile on rock surfaces of Khao Khad limestone after CAI testing for three joints. Arrow indicates scratching direction.

Phu Phan sandstone, J_n = 3

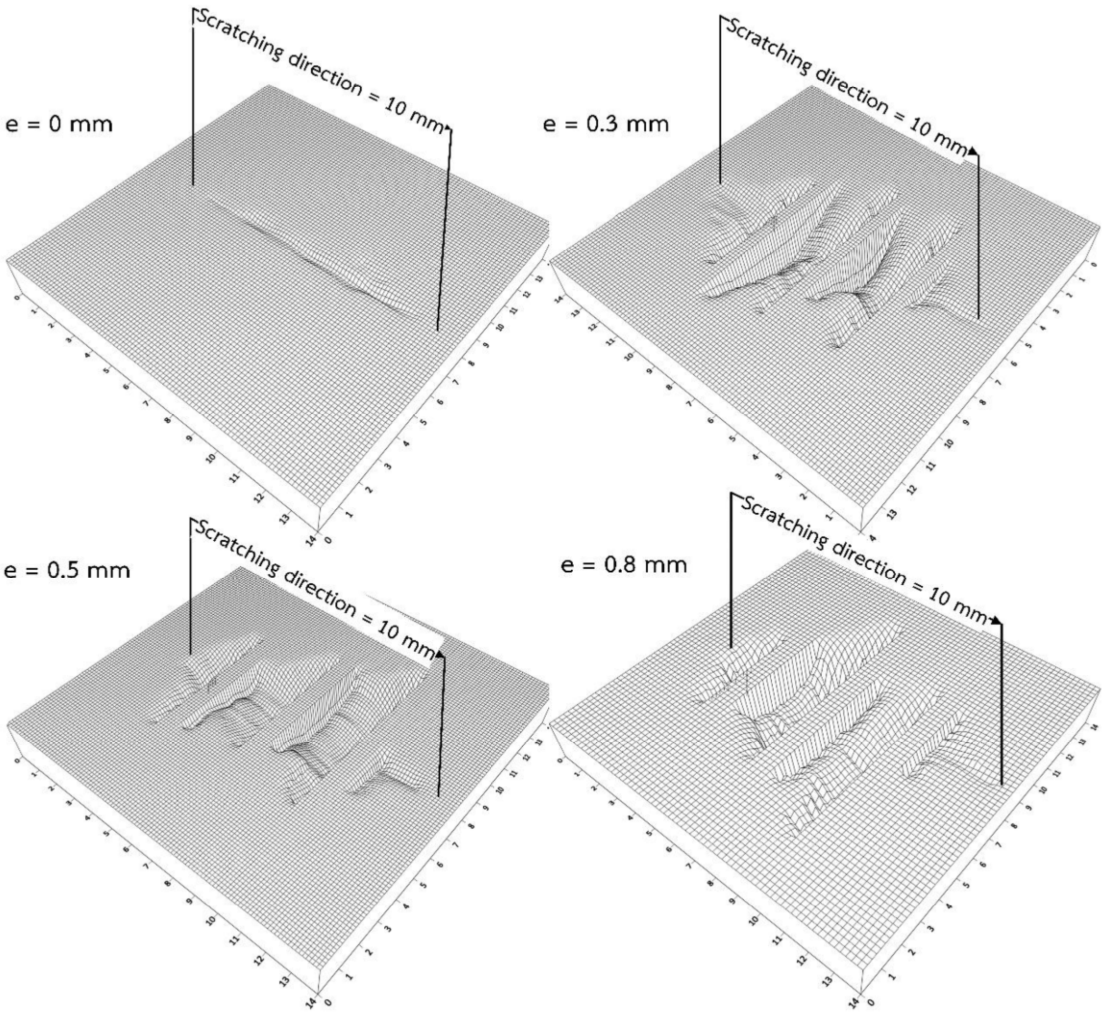

Figure G.9 Example of scratching groove profile on rock surfaces of Phu Phan sandstone after CAI testing for three joints. Arrow indicates scratching direction.

Buriram basalt, J_n = 3

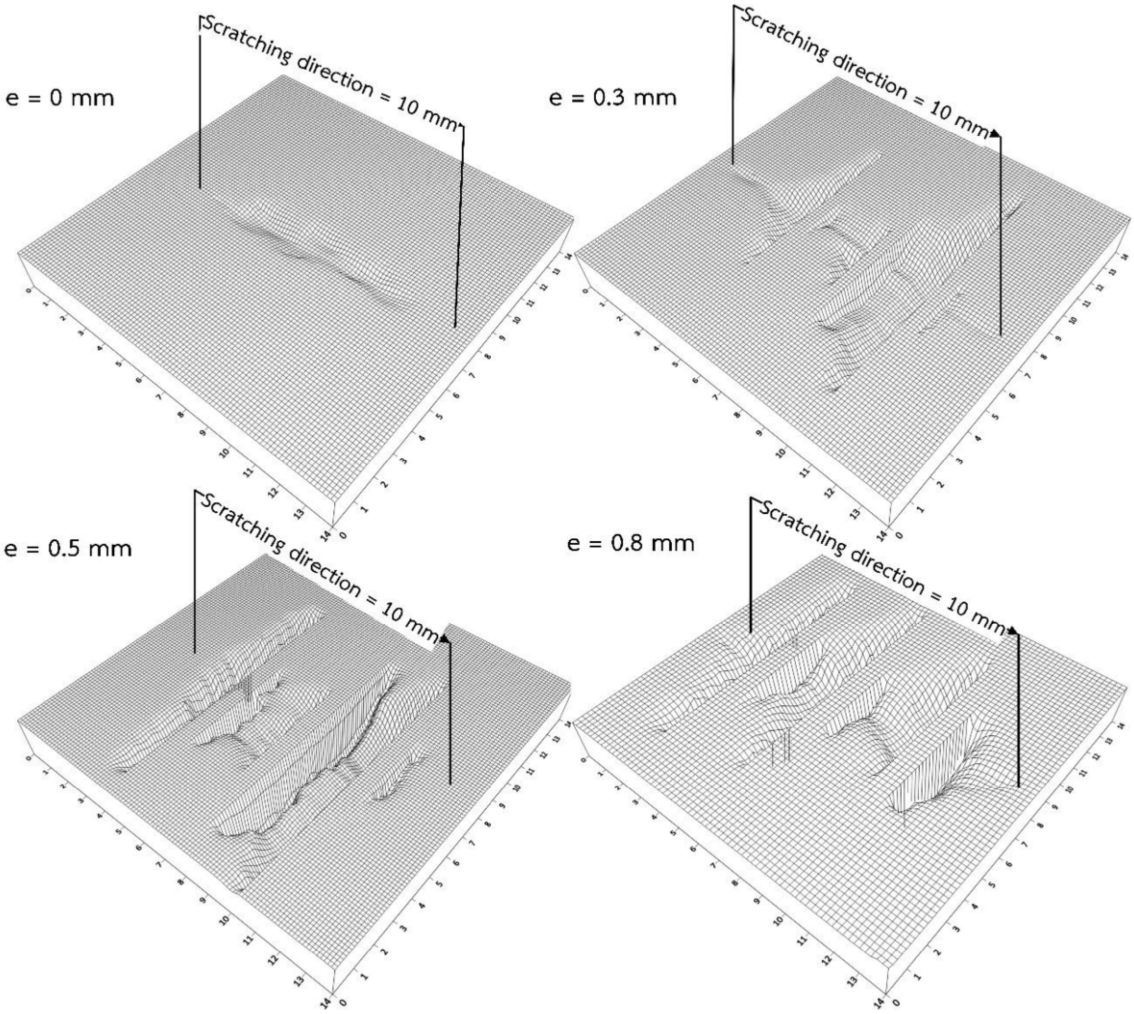

Figure G.10 Example of scratching groove profile on rock surfaces of Buriram basalt after CAI testing for three joints. Arrow indicates scratching direction.

Khao Khad limestone, J_n = 4

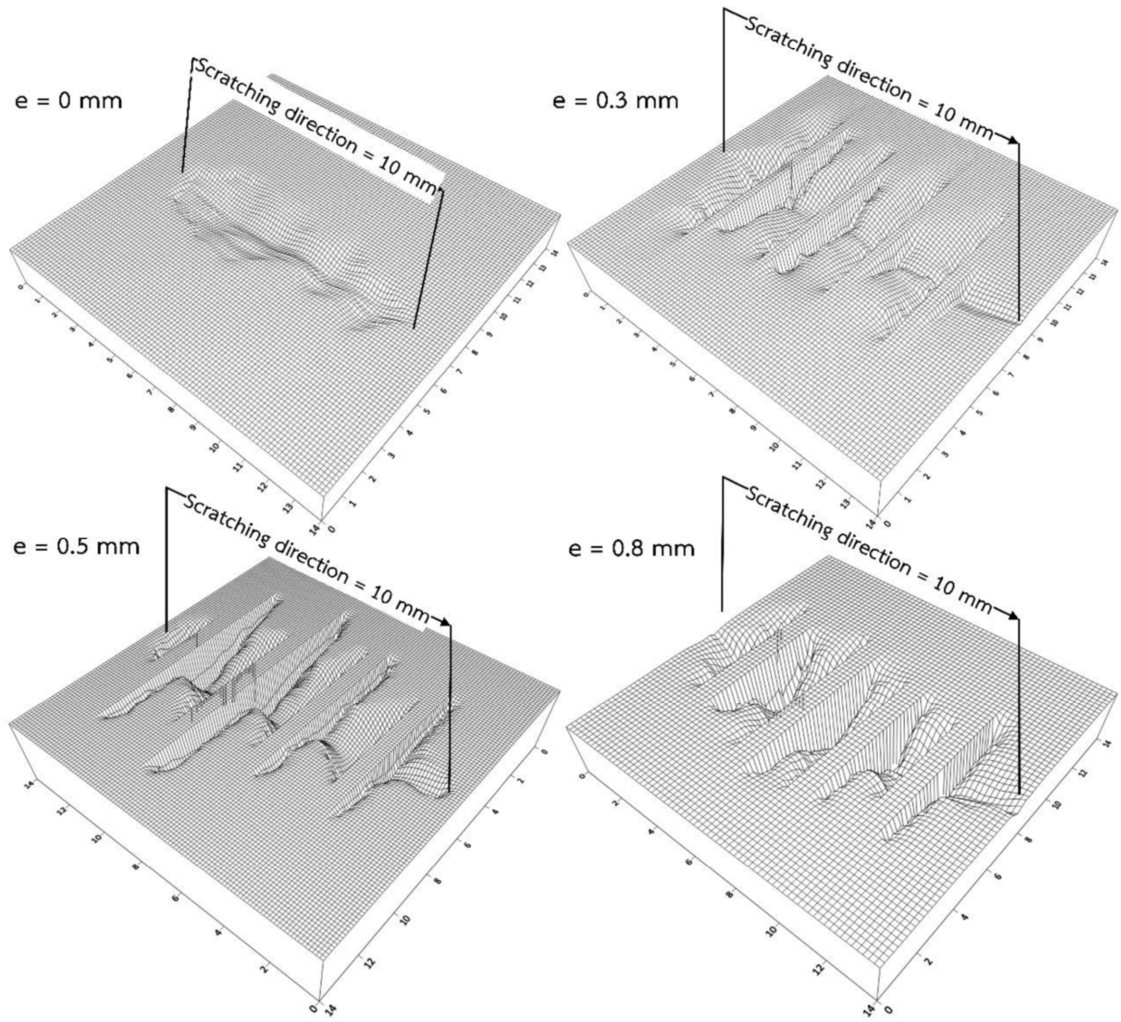

Figure G.11 Example of scratching groove profile on rock surfaces of Khao Khad limestone after CAI testing for four joints. Arrow indicates scratching direction.

Phu Phan sandstone, J_n = 4

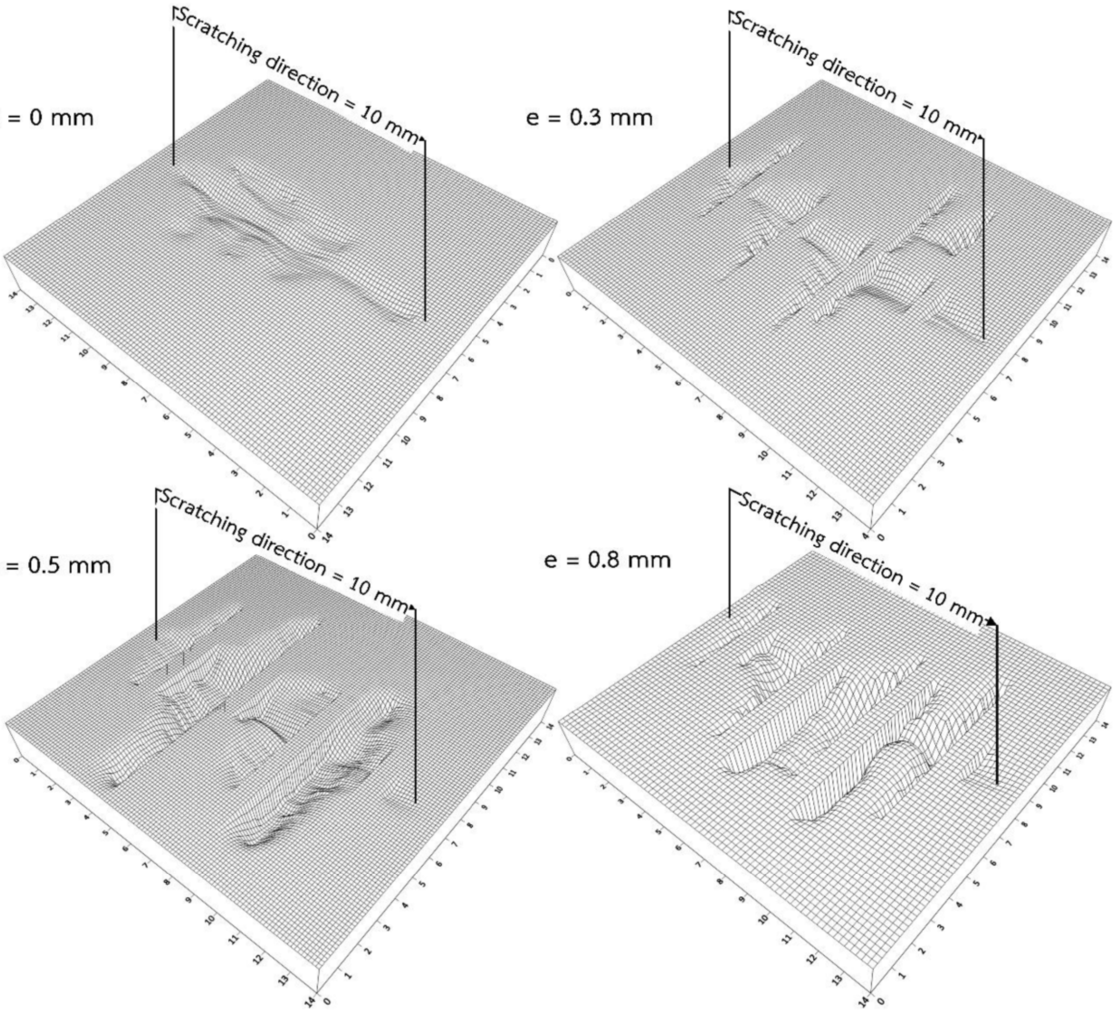

Figure G.12 Example of scratching groove profile on rock surfaces of Phu Phan sandstone after CAI testing for four joints. Arrow indicates scratching direction.

Buriram basalt, J_n = 4

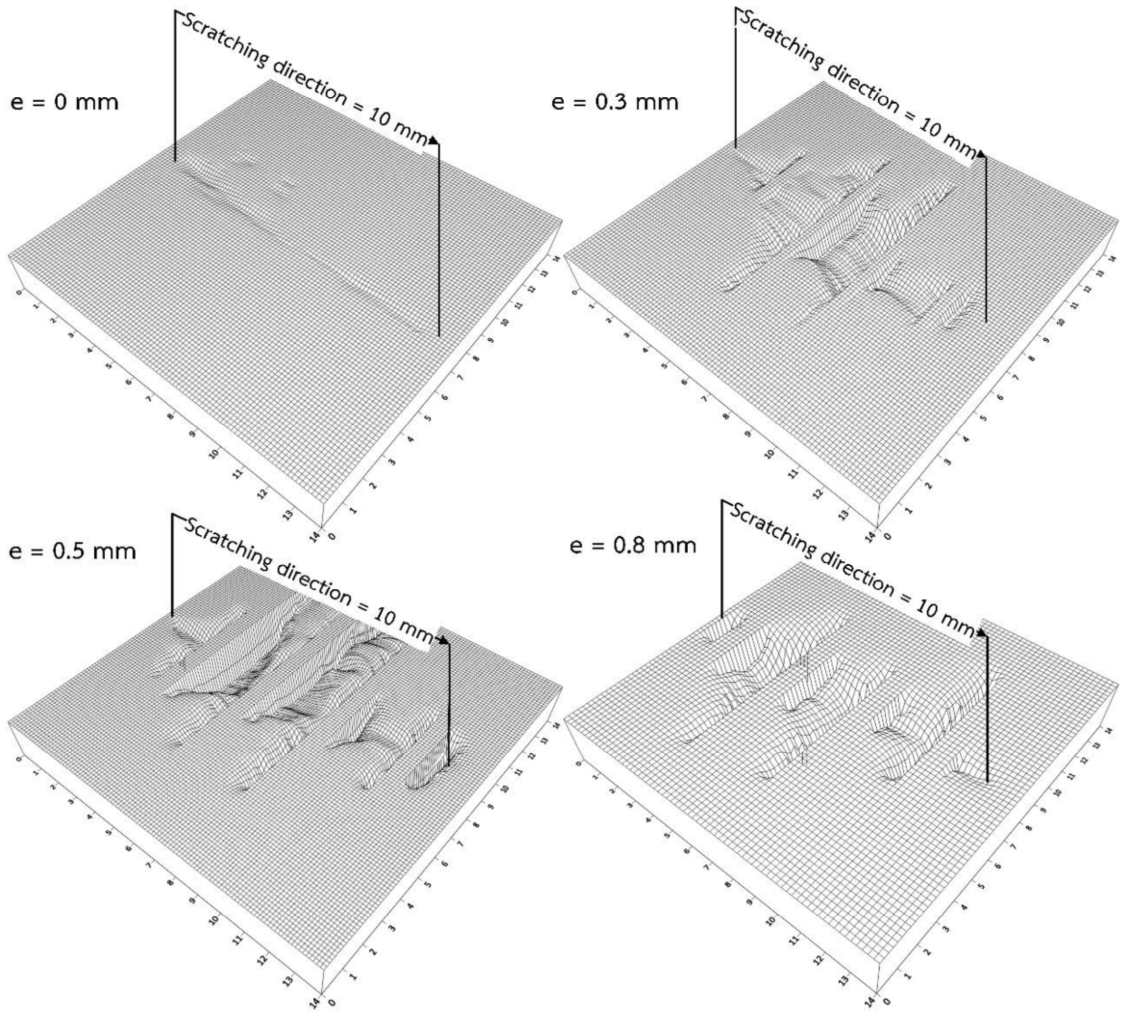

Figure G.13 Example of scratching groove profile on rock surfaces of Buriram basalt after CAI testing for four joints. Arrow indicates scratching direction.

APPENDIX H

LIST OF PUBLICATION

Effect of Rock Joint Frequency and Aperture on CERCHAR Abrasivity Index

Ratchapon Mingkhwan(✉), Thanittha Thongprapha, Laksikar Sitthimongkol, and Kittitep Fuenkajorn

Geomechanics Research Unit, Suranaree University of Technology, 111 University Avenue, Nakhon Ratchasima 30000, Thailand
M6500801@g.sut.ac.th

Abstract. The objective of this study is to investigate the effect of rock joints on the CERCHAR abrasivity index (CAI). Sandstone, limestone, and basalt with parallel fractures with joint numbers varying from 1, 2, 3, to 4, and joint apertures of 0, 0.3, 0.5, to 0.8 mm are tested. The joint spacing is kept constant at 2 mm. The results indicate that the CAI value decreases with increasing joint frequencies and apertures. The ploughing force exerted on the stylus pin is reduced when the pin tip reaches the fracture. This becomes more pronounced as the aperture becomes larger. As the number of joints increases and the separations widen, greater scratching force is increased. The ploughing volume increases as CAI decreases, suggesting that highly fractured rocks show less CAI and less energy to cut while yielding a higher ploughing volume as compared to rock with less fractures.

Keywords: joint number · joint separation · ploughing force · ploughing volume

1 Introduction

Rock abrasiveness is an important factor influencing the performance and longevity of excavation tools leading to significant costs associated with wear and tear. The effectiveness of excavation tools on-site is affected by various rock characteristics, making it essential to gather detailed information about the rock properties in the area before starting any work [1]. Rock abrasiveness is determined by the type of rock and the presence of abrasive minerals within it. As a result, several tests have been developed and widely used for rock identification [2]. Since a huge portion of excavation budget is spent on repair and costly replacement of rock cutting tools which results in time loss [3, 4].

CERCHAR abrasivity index (CAI) is a widely used test for evaluating the abrasion resistance of drill bits. Its popularity is attributed to the method's simplicity, speed, and low cost [5–7], which has driven extensive research to obtain various practical outcomes. The relationship of the CERCHAR abrasivity index (CAI) with various factors has been extensively researched, including testing length [8–10], velocity [11–13], surface conditions [9, 14], mineral and rock composition [15], orientation [16], temperature [17] and mechanical properties [4, 17–19].

T. Kang and Y. Lee (Eds.): ICCEA 2024, LNCE 640, pp. 368–376, 2025.
https://doi.org/10.1007/978-981-96-6115-2_31

Despite the extensive research conducted on the CAI, the current understanding does not fully account for all the variables that influence CAI. Specifically, the effects of number of joints and their aperture width in rock are critical but have not been thoroughly explored. This test introduces a new concept that is an important factor in affecting CAI when observing tool wear. For example when a drill bit encounters a rock formation with a greater number of joints or wide apertures, these structural features can significantly affect the drill bit performance, potentially leading to increased wear or altered drilling efficiency. Understanding these effects is essential for improving the accuracy of CAI as a predictive tool and for optimizing drilling operations in geologically complex environments.

The objective of this study is to assess the effect of rock joints on CAI. Number of joints and their apertures are considered. Three rock types have been tested. Methematical relations between CAI and joint characteristics are developed.

2 Sample Preparation

Three rock types have been used in this study including Khao Khad limestone, Phu Phan sandstone and Buriram basalt. They widely exposed in the northeast of Thailand. The rock specimens are cut and ground to produce saw-cut surface in accordance with the ASTM D7625–22 standard practice. Rectangular block specimen with nominal dimensions of $80 \times 50 \times 40$ mm^3 are obtained with artificial fractures (saw-cut) normal to the test surfaces. The numbers of parallel joints are varied from 1 to 4, with joint apertures from 0 to 0.8 mm. The joint apertures are made by using filler gages placed between thin slaps of rock specimens to obtain a precise gap (aperture) between them. These thin slaps are then glued together while maintaining the desired joint apertures and spacing.

3 Test Method

The CERCHAR abrasivity test follows the ASTM D7625–22 standard practice with an apparatus similar to the West apparatus (Fig. 1). Five scratching lines are made perpendicular to joint aperture (Fig. 2).

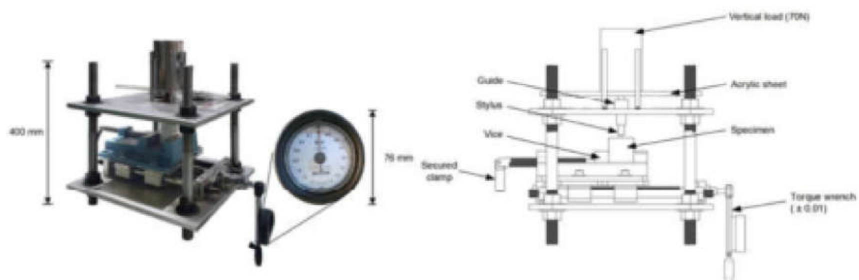

Fig. 1. Device based on West CERCHAR apparatus [20] with additional torque [13].

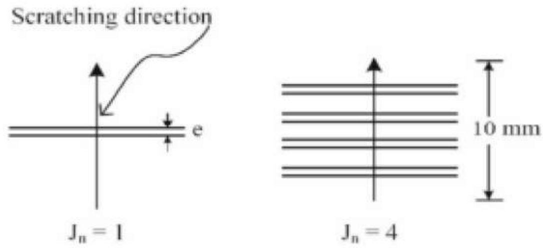

Fig. 2. Scratching direction perpendicular to joints with $J_n = 1$ to 4 and e = 0, 0.3, 0.5 to 0.8 mm.

The ploughing force during scratching is measured by a torque meter to calculate the scratching energy, which is affected by different joint characteristics. The force can be calculated using the following equation [13]:

$$F = 2\pi T/P \quad (1)$$

where F is ploughing force (N), T is torque (N•m) and P is screw pitch (0.001 m). The rock surface after CAI testing have been laser-scanned to observe groove shape and to calculate the groove volume. The measurements are made to the nearest 0.001 mm.

4 Test Results

4.1 Correlation Between CAI and Rock Joint Characteristics

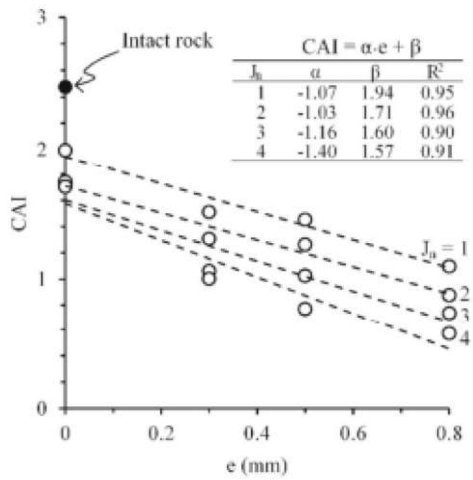

Fig. 3. CAI as a function of joint aperture (e) for different numbers of joints (J_n) for Buriram basalt.

Result of the CAI tests are shown in Table 1. The CAI value of Buriram basalt tends to decrease with increasing number of joints (J_n) and aperture (e) (Fig. 3). This is true for all rock types. This is because the stylus contacts the rock surface less frequently when larger gaps (apertures) are present within a 10 mm scratching length, leading to less abrasion. A linear equation is proposed to present relationship between CAI and joint aperture, as follows;

$$\mathrm{CAI} = \alpha \cdot e + \beta \tag{2}$$

where α and β are empirical constants, and e is joint aperture. Good correlations are obtained ($R^2 > 0.9$). Table 1 gives these empirical constants for all tested rocks.

4.2 Correlation Between Force and Rock Joint Characteristics

Figure 4 shows example of scratching force as a function of distance for limestone. The force (F) increases with scratching displacement (d_s) and number of joints. Rock with higher number of joints and aperture requires greater ploughing force as compared to those with fewer joints. Joint apertures show more effect on the ploughing force than does number of joints. The correlation between F-ds can be described by an exponential equation [15], as follows:

$$F = a \cdot [1 - \exp \cdot (-b \cdot d_s)] \tag{3}$$

where a and b are empirical constants, good correlation is obtained ($R^2 > 0.9$). Table 1 summarizes the result for the three rock types.

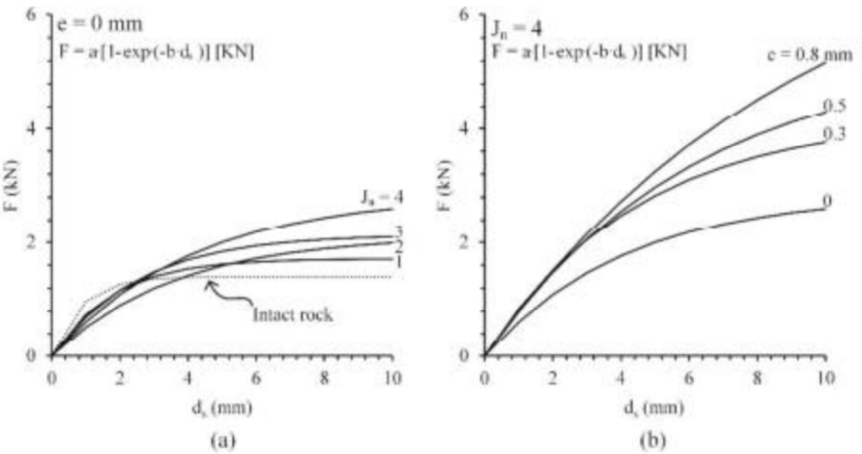

Fig. 4. Scratching force as a function of distance for joint aperture (e) = 0 mm under different numbers of joints (a), and under $J_n = 4$ with different apertures (b) for Khao Khad limestone.

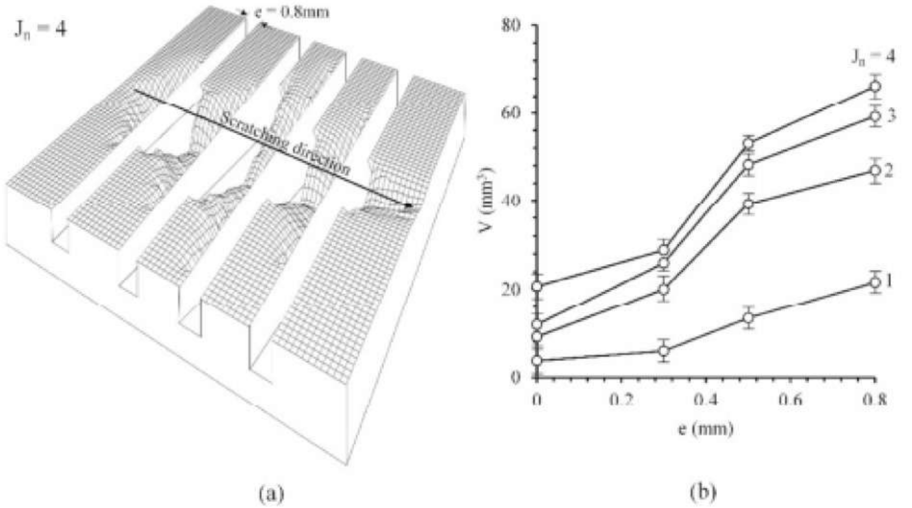

Fig. 5. Example of scratching groove profile of sandstone with $J_n = 4$ (a), and groove volume as a function of joint aperture with different J_n values (b) for sandstone.

4.3 Correlation Between Groove Volume and Rock Joint Characteristics

Figure 5a shows that the groove volume of material scratched increases as the stylus approaches joints. This increase is attributed to the reduced rock surface area before the material fails under the applied load force, leading to a larger groove volume of material being removed along the joint. Figure 5b shows that the groove volume of the scratched area increases with joint aperture (e). A larger e, which may correspond to increased Jn or e, results in a greater groove volume of material being scratched out.

The CAI values decrease as a result of both J_n and e. This reduction is attributed to the stylus tip entering the joint apertures during the test, which led to a smaller abrasion of the stylus. The stylus tip did not maintain contact with the entire rock surface over the 10 mm distance, resulting in reduced overall abrasion.

Sandstone and basalt show higher CAI values than limestone. This may be due to the dependence of CAI on rock strength, as indicated by previous studies [14, 15], which report strengths of 81.43 MPa for sandstone, 79.17 MPa for basalt and 54.61 MPa for limestone. Hard rock gives greater CAI values and more affected by joint characteristics than softer ones.

The force measured during the CAI increases with Jn and e. Higher numbers of joints and larger apertures required higher force to scratch the rock surface. This is attributed to the stylus encountering the gaps created by larger apertures, with additional resistance. This is because when the stylus passes through a large gap, it drops and requires more force to step up to continue scratching.

Table 1. CERCHAR abrasivity index, force and groove volume for all rocks.

Rock type	J_n	e	CAI	CAI = α•e + β		F = a · [1 - exp · (-b · d_s)]		V
		(mm)		α (mm^{-1})	β	a (N)	b (mm^{-1})	(mm^3)
Khao Khad limestone	0	–	1.75			1.40	1.19	1.14
		0	1.47			1.78	0.56	1.12
	1	0.3	1.37	−0.65	1.51	3.21	0.32	3.01
		0.5	1.17			3.81	0.28	11.78
		0.8	0.96			4.64	0.20	16.05
		0	1.36			2.11	0.27	1.92
	2	0.3	1.13	−0.52	1.32	5.56	0.11	10.36
		0.5	1.02			14.08	0.04	21.05
		0.8	0.94			12.50	0.05	32.74
		0	1.25			2.13	0.39	5.25
	3	0.3	1.10	−0.63	1.27	4.80	0.17	16.90
		0.5	0.95			5.20	0.16	40.44
		0.8	0.75			4.45	0.28	50.99
		0	0.97			2.86	0.23	14.71
	4	0.3	0.95	−0.35	1.00	4.22	0.22	20.26
		0.5	0.80			5.37	0.16	47.65
		0.8	0.71			7.96	0.10	54.63
Phu Phan sandstone	0	–	2.27			1.54	1.05	1.58
		0	1.63			1.51	1.34	3.68
	1	0.3	1.56	−0.80	1.67	1.86	0.63	5.89
		0.5	1.20			2.16	0.44	13.34
		0.8	1.04			2.58	0.61	21.61
		0	1.41			2.43	0.64	9.09
	2	0.3	1.08	−0.71	1.36	3.96	0.17	20.03
		0.5	0.96			4.53	0.16	39.21
		0.8	0.83			4.72	0.17	46.92
		0	1.34			2.66	0.70	11.87
	3	0.3	0.95	−0.73	1.27	10.26	0.07	25.95
		0.5	0.88			10.86	0.07	48.20

(continued)

Table 1. (*continued*)

Rock type	J_n	e	CAI	CAI = α•e + β		F = a · [1 - exp · (-b · d_s)]		V
		(mm)		α (mm^{-1})	β	a (N)	b (mm^{-1})	(mm^3)
		0.8	0.73			12.81	0.06	59.19
		0	1.23			2.78	0.75	20.67
	4	0.3	0.72	−0.81	1.12	11.11	0.03	28.81
		0.5	0.69			19.26	0.04	52.99
		0.8	0.57			186.45	0.09	66.31
Buriram basalt	0	–	2.47			2.06	0.42	3.08
		0	1.99			2.14	0.47	0.85
	1	0.3	1.51	−1.07	1.94	3.11	0.27	2.87
		0.5	1.45			4.58	0.16	10.75
		0.8	1.09			5.76	0.12	13.78
		0	1.74			1.89	0.46	2.49
	2	0.3	1.0	−1.03	1.71	4.12	0.18	11.02
		0.5	1.26			6.57	0.09	29.16
		0.8	1.87			9.24	0.08	38.15
		0	1.71			4.12	0.16	3.89
	3	0.3	1.06	−1.16	1.60	5.21	0.16	14.87
		0.5	1.02			6.88	0.12	34.60
		0.8	0.87			6.44	0.16	47.72
		0	1.70			3.57	0.23	13.85
	4	0.3	1.00	−1.40	1.57	6.30	0.16	18.37
		0.5	0.77			7.26	0.16	42.57
		0.8	0.57			8.22	0.14	51.21

5 Discussions

The results obtained here are limited to the condition at which the scratching direction is only normal to the joint lines with one joint set. The effect of the angles between scratching direction and joint line has not been investigated.

6 Conclusion

The results obtained here can be concluded as follows.

- Number of joint and aperture can decrease the wear of stylus pin (CAI) while

- The effects of joint aperture and joint number on CAI and ploughing force pronounce more in strong rock (basalt) than in soft rock (limestone).
- The groove volume increases more rapidly for larger numbers of joints, as compared to smaller number of joints.
- The effect of joint aperture on groove volume is more significant in soft rock than in the stronger one.

References

Thuro, K., Käsling, H.: Classification of the abrasiveness of soil and rock. Geomechanics Tunnelling. **2**(2), 179–188 (2009)

Ghasemi, A.: Study of CERCHAR abrasivity index and potential modifications for more consistent measurement of rock abrasion. Master Thesis, Pennsylvania State University (2010)

Fowell, R.J., Bakar, A.M.Z.: A review of the CERCHAR and LCPC rock abrasivity measurement methods. In: Proceeding of the 11th Congress of the International Society for Rock Mechanics, pp. 155–160 (2007)

Hamzaban, M.T., Memarian, H., Rostami, J.: Continuous monitoring of pin tip wear and penetration into rock surface using a new Cerchar abrasivity testing device. Rock Mech. Rock Eng. **47**(2), 689–701 (2014)

Prieto, L.A.: The CERCHAR abrasivity index's applicability to dredging rock. In: Proceedings of Western Dredging Association (WEDA XXXII) Technical Conference and Texas A&M University (TAMU 43) Dredging Seminar; San Antonio, Texas, pp. 212–9 .June 10–13 (2012)

Ko, T.Y., Kim, T.K., Son, Y., Jeon, S.: Effect of geomechanical properties on CERCHAR abrasivity Index (CAI) and its application to TBM tunnelling. Tunnel Underground Space Technol. **57**, 99–111 (2016)

Hamzaban, M.T., Karami, B., Rostami, J.: Effect of pin speed on CERCHAR abrasion test results. J. Test. Eval. **47**(1), 121–39 (2019)

Al-Ameen, S.I., Waller, M.D.: The influence of rock strength and abrasive mineral content on the Cerchar abrasive index. Eng. Geol. **36**(3–4), 293–301 (1994)

Plinninger, R., Käsling, H., Thuro, K., Spaun, G.: Testing conditions and geomechanical properties influencing the CERCHAR abrasiveness index (CAI) value. Int. J. Rock Mech. Min. Sci. **40**(2), 259–263 (2003)

Yaralı, O., Duru, H.: Investigation into effect of scratch length and surface condition on Cerchar abrasivity index. Tunn. Undergr. Space Technol. **60**(36), 111–120 (2016)

Kotsombat, T., Thongprapha, T., Fuenkajorn, K.: Scratching rate effects on cerchar abrasiveness index of sandstones. In: Academicsera International Conference, Chiang Mai, Thailand, pp. 6–9 (2020)

Plinninger, R. J., Kasling, H., Thuro, K.: Wear prediction in hardrock excavation using the CERCHAR abrasiveness index (CAI). EUROCK 2004 & 53rd Geomechanics Colloquium. Schubert (ed.). pp. 1–6 (2004)

Rostami, J., Ghasemi, A., Alavi Gharahbagh, E., Dogruoz, C., Dahl, F.: Study of dominant factors affecting Cerchar abrasivity index. Rock Mech. Rock Eng. **47**, 1905–1919 (2014)

Thanadkha, P., Fuenkajorn, K.: Correlation between cerchar abrasivity index of smooth and rough rock fractures. In: Academicsera International Conference, Kuala Lumpur, Malaysia, pp. 8–12 (2022)

Kathancharoen, N., Fuenkajorn, K.: Effects of mechanical and mineralogical properties on cerchar abrasivity index and specific energy of some Thai rocks. Eng. Appl. Sci. Res. **50**(5), 478–489 (2023)

Alber, M., Yarali, O., Dahl, F., et al.: ISRM suggested method for determining the abrasivity of rock by the CERCHAR abrasivity test. In: Ulusay R (ed) The ISRM suggested methods for rock characterization, testing and monitoring, Springer, 2007–2014, Publishing, Cham, pp. 101–106 (2015)

Ji, Y., Wang, L., Zheng, Y., Wu, W.: Temperature-dependent abrasivity of Bukit Timah granite and implications for drill bit wear in thermomechanical drilling. Acta Geotech (2020)

Capik, M., Yilmaz, A.O.: Correlation between Cerchar abrasivity index, rock properties, and drill bit lifetime. Arab. J. Geosci. **10**(15), 1–12 (2017)

Alber, M.: Stress dependency of the Cerchar abrasivity index (CAI) and its effects on wear of selected rock cutting tools. Tunn. Undergr. Space Technol. **23**(4), 351–359 (2008)

Deliormanlı, A.H.: Cerchar abrasivity index (CAI) and its relation to strength and abrasion test methods for marble stones. Constr. Build. Mater. **30**, 16–21 (2012)

West, G.: Rock abrasiveness testing for tunnelling. Int. J. Rock Mech. Min. Sci. Geomech. Abstracts **26**(2), 151–160 (1989)